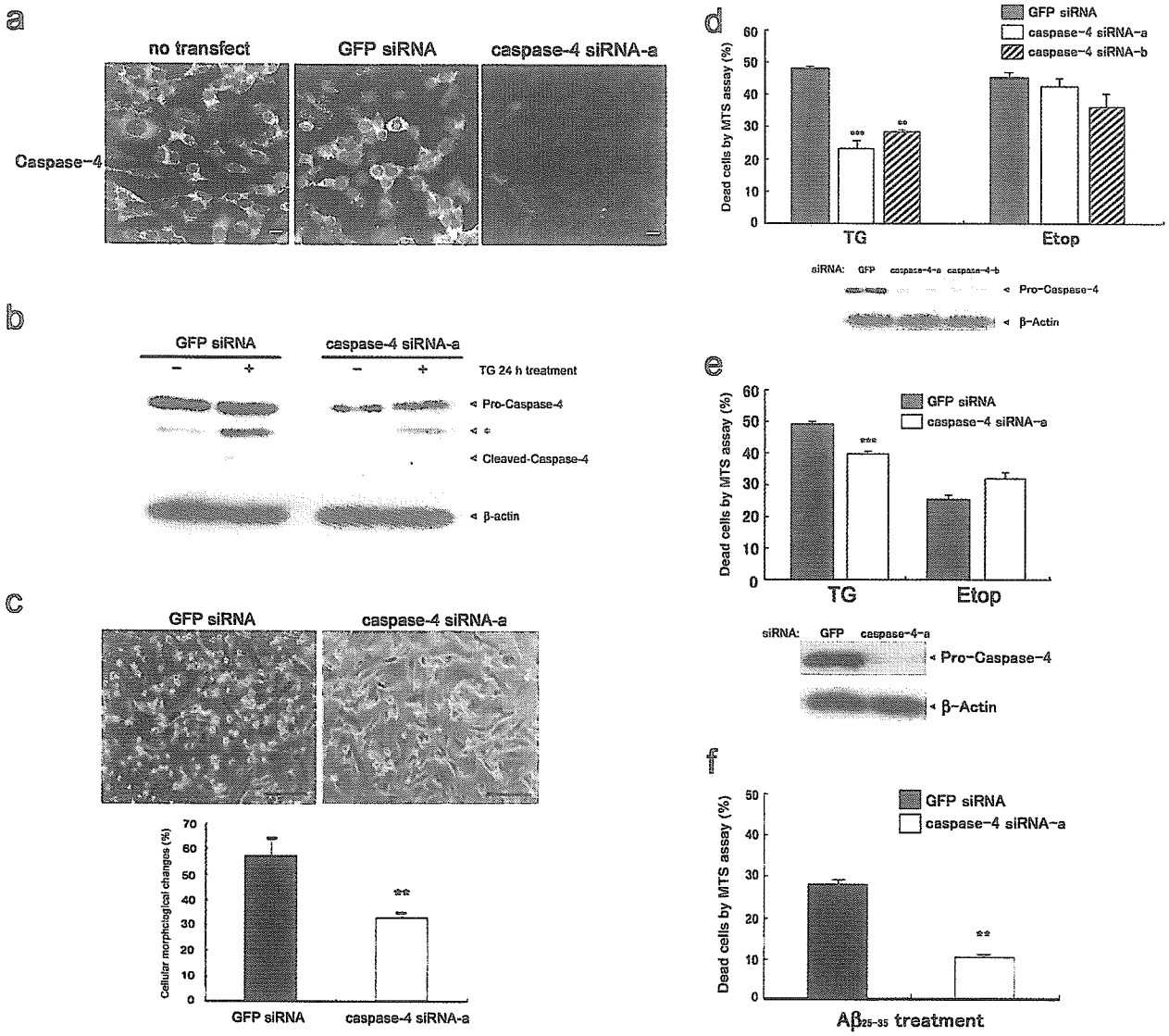

Figure 4. **Decrease in ER stress- or Aβ-induced cell death after siRNA-mediated reduction of caspase-4 expression.** (a) SK-N-SH cells were transfected with siRNA oligos (1 μg oligo/24 well plate) to GFP (control) or caspase-4 (siRNA-a). After incubation for 60 h, cells were fixed and stained with caspase-4 antibodies as described in Materials and methods. Bars, 5 μm. (b) Cells were transfected as in panel a. After incubation for 60 h, cells were incubated with (+) or without (−) 0.5 μM thapsigargin for 24 h. Equal amounts of cell lysates (10 μg) were analyzed by Western blotting using anti–caspase-4 antibody (top) or anti–β-actin antibody (bottom). (c) Top panels show representative phase-contrast images of GFP siRNA-transfected cells (left) and caspase-4 siRNA-a–transfected cells (right) after treatment with 0.5 μM thapsigargin for 40 h. The bottom panel shows the extent of cell death assessed by morphological changes, and expressed as the mean ± SEM for three independent experiments as described in Materials and methods. Asterisks show a significant difference from controls (GFP siRNA-transfected cells): **, indicates $P < 0.01$. Bars, 50 μm. (d) Cells were transfected with the indicated siRNAs, and cell viability after 0.5 μM thapsigargin or 100 μM etoposide treatment for 40 h was estimated by the MTS assay. Results were expressed as the mean ± SEM for three independent experiments. Asterisks show a significant difference from controls: **, indicates $P < 0.01$; ***, indicates $P < 0.001$. Bottom panel shows reduction of caspase-4 level by the indicated siRNAs assessed by Western blotting as described in panel b. (e) HeLa cells were transfected with GFP siRNA or caspase-4 siRNA-a as described in Materials and methods. After incubation for 24 h, cells were incubated with 0.5 μM thapsigargin for 40 h, and then viability was estimated as described in panel d. Each value represents the mean ± SEM for three independent experiments. Asterisks show a significant difference from controls: ***, indicates $P < 0.001$. (f) SK-N-SH cells were transfected with GFP siRNA or caspase-4 siRNA-a. After incubation for 60 h, cells were incubated with 25 μM $A\beta_{25\text{-}35}$ peptide for 40 h, and then viability was estimated as described in panel d. Each value represents the mean ± SEM for three independent experiments. Asterisks show a significant difference from controls: **, indicates $P < 0.01$.

is essential for the activation of caspase-1/ICE to promote pro–IL-1β (interleukin-1β) processing (Wang et al., 1996, 1998). On the other hand, caspase-5 is likely involved in processing of pro–IL-1β together with caspase-1/ICE (Martinon et al., 2002) and the caspase-5 gene resembles the mouse caspase-11 in its lipopolysaccharide inducibility (Lin et al., 2000). Therefore, caspase-5 should be the orthologue of caspase-11. Here, the screening process yielded the caspase-4 gene as the homologous gene to mouse caspase-12. Thus, caspase-4 is the best candidate that would function similarly to mouse caspase-12 in ER stress-induced cell death in humans.

Here, we examined the localization of human caspase-4 using several methods. The immunostaining analysis using anti–caspase-4 antibody and fluorescent analysis for caspase-4/GFP fusion protein in Fig. 1 showed the predominant localization of caspase-4 on the ER. On the other hand, the immuno-EM showed the nearly equal distribution of caspase-4 on the ER and mitochondria, and subcellular fractionation showed that caspase-4 was recovered in the microsome-enriched and mitochondria-enriched fractions, and also in cytosolic fraction. Although we could not eliminate contamination of ER marker proteins in the mitochondria-enriched fraction in subcellular fractionation using SK-N-SH cells, microsome-enriched fraction does not seem to contain mitochondria and cytosol. Under these conditions, caspase-4 was recovered in both mitochondria-enriched fraction and microsome-enriched fraction, and amounts of caspase-4 recovered in the microsome-enriched and mitochondria-enriched fractions were comparable to those of ER marker, presenilin-1. Therefore, considering all the results shown in Fig. 1, we concluded that caspase-4 was localized to the ER membrane, and probably to the mitochondria in addition.

Caspase-4 on the ER is supposed to function in ER stress-induced apoptosis similarly to caspase-12. In supporting this hypothesis, caspase-4 was cleaved specifically by ER stress and Aβ-treatment, but not by other apoptotic stimuli including etoposide, staurosporine, and UV. Additionally because Bcl-2 that can completely inhibit the signaling pathway at least downstream from mitochondria, did not prevent the cleavage of caspase-4 by ER stress, it should be most probable that caspase-4 on the ER but not on mitochondria is primarily cleaved. We also showed that reduction of the level of caspase-4 by RNA interference (RNAi) resulted in decrease in ER stress-induced cell death and Aβ-induced cell death, but did not affect cell death induced by etoposide. The characteristics of human caspase-4 shown here are very similar to those of mouse caspase-12 reported previously (Nakagawa et al., 2000), and therefore, caspase-4 is able to substitute the caspase-12 functions in ER stress-induced apoptosis and Aβ-induced cell death. Because caspase-4 was also localized to the mitochondria in addition to the ER membrane, whereas caspase-12 was shown to localize predominantly to the ER, but not to the mitochondria (Nakagawa et al., 2000), caspase-4 might have additional function compared with caspase-12, although the function of caspase-4 on mitochondria is not clear.

Several mechanisms that activate caspase-12 have been proposed in mouse system. For example, calpain, a protease that can be activated by calcium released from ER upon ER stress, starts cleavage of caspase-12 (Nakagawa and Yuan, 2000), caspase-7 activates caspase-12 upon prolonged ER stress (Rao et al., 2001), or TRAF2 mediates caspase-12 activation, which is regulated by IRE1α (Yoneda et al., 2001). It is not clear which mechanism is involved in activation of caspase-4, but because final cleavage products were not observed in cells with activated caspase-7 (Fig. 2 a), activation of caspase-7 does not seem to be enough for full activation of caspase-4. To know the precise mechanism that activate caspase-4, it should be important to find proteins that interact with pro–caspase-4 during ER stress-induced apoptosis.

The inhibition of apoptosis induced by ER stress exposure by RNAi to caspase-4 was incomplete. It is possible that the residual activity of caspase-4 after RNAi would be responsible for the cell death. Alternatively, other apoptotic mechanisms might also operate simultaneously. Several possible pathways have been postulated for ER stress-induced apoptosis. ER stress is reported to activate ASK–c-Jun NH_2-terminal kinase pathway through the IRE1–TRAF2–ASK1 complex formation (Nishitoh et al., 2002). Other signaling pathway is mediated by transcriptional activation of genes encoding proapoptotic function. Activation of stress transducer IRE1, PERK, or ATF6 leads to transcriptional activation of CHOP/GADD153, a bZIP transcription factor that potentiates apoptosis (Oyadomari et al., 2002). Operation of these mechanisms might account for incomplete inhibition of ER stress-induced apoptosis by knockout of caspase-12 and knockdown of caspase-4 in mouse and humans, respectively. It is possible that caspase-dependent mechanism and other mechanisms function in parallel in initiating ER stress-induced apoptosis, and the mechanism that mainly operates could differ depending on cell types. We have shown that the extent to decrease in cell death by decreasing caspase-4 level of SK-N-SH cells was comparable to that reported for caspase-12 knockout mouse (Nakagawa et al., 2000), whereas that of HeLa cells was relatively less. We also find some cells, like HUVEC, in which decrease in caspase-4 did not affect the ER stress-induced apoptosis (unpublished data). Thus, caspase-4 has been shown to function in ER stress-induced apoptosis at least in several cell lines, including SK-N-SH and HeLa cells, but not all cells.

Cell death caused by Aβ treatment was also partially inhibited by RNAi to caspase-4. Although it is controversial whether Aβ-induced cell death involves ER stress-induced apoptosis, the results are consistent that these two types of cell death are mediated by common mechanism at least in part. Recent report described that the cell death induced by Aβ was inhibited by the broad-spectrum caspase inhibitor z-VAD and more specifically by the down-regulation of caspase-2 with antisense oligonucleotides (Haviv et al., 1998). Neuronal culture derived from caspase-2 null mice was also shown to be partially resistant to $A\beta_{1\text{-}42}$ toxicity (Troy et al., 2000). Thus $A\beta_{1\text{-}42}$-induced cell death might be mediated by caspase-2 as well as caspase-12. It is possible that both caspases 2 and 4 are involved in Aβ-induced cell death also in the human system.

Because caspase-4 seems to be responsible for cell death after Aβ treatment, caspase-4 might be involved in pathogenesis of AD. Consistently to this hypothesis, our preliminary analysis showed an increase in cytoplasmic staining for caspase-4 in the pyramidal cell layer of the hippocampal CA1-2 region in AD patients, but not in control brains (unpublished data). All of the AD brains tested had stronger caspase-4 immunoreactivity than disease control brains from patients with other neurodegenerative disorders ($n = 4$ for AD and $n = 3$ for disease control), and the strong staining was remarkable in the pyramidal neurons around deposits of β-amyloid. Increased caspase-4 might elevate the vulnerability of neurons to apoptosis, and therefore may be involved in the pathogenesis of AD.

Bcl-2 family proteins play essential roles in regulating apoptosis. Although antiapoptotic family members (Bcl-2, Bcl-x_L) and multidomain proapoptotic members (Bak, Bax) are thought to function mainly on mitochondria, recent studies suggest that they may also function on the ER where they reside as well. Overexpression of Bcl-2 (Foyouzi-Youssefi et al., 2000; Pinton et al., 2000) or knockout of both Bak and Bax (Scorrano et al., 2003) are reported to reduce ER Ca^{2+} concentration, but other reports showed that Bcl-2 enhanced the retention of Ca^{2+} in the ER lumen (Distelhorst et al., 1996; He et al., 1997). Thus, although it is still controversial, Bcl-2 family members may contribute to regulating ER stress-induced apoptosis on the ER (Ferri and Kroemer, 2001; Scorrano et al., 2003; Zong et al., 2003) in addition to their main function on mitochondria. Our results demonstrate that overexpressed Bcl-2 and Bcl-x_L, which can completely inhibit the signaling pathway at least downstream from mitochondria, did not prevent, but slightly affected, the cleavage of caspase-4 by ER stress. The slight decrease might be due to the absence of its feed back cleavage by downstream effector caspases, such as caspase-3. Therefore, without regard to the mitochondria or the ER where Bcl-2 family functions, activation of caspase-4 should be the primary reaction in ER stress-induced activation of caspases.

In this work, we discovered that caspase-4 plays a key role in ER stress-induced apoptosis in humans. Caspase-4 also seems to act in the β-amyloid–induced cell death, suggesting that human caspase-4 corresponds to rodent caspase-12 to initiate cell death signaling pathway, and that the activation of caspase-4 would mediate neuronal cell death in neurodegenerative disorder. Caspase-4 could be the potential target to develop treatments for such diseases including AD.

Materials and methods

Chemicals and antibodies

We used the following antibodies: anti–caspase-4 mAb (4B9; MBL International Corporation), anti–caspase-4 pAb (Santa Cruz Biotechnology, Inc.), anti-KDEL mAb (10C3; StressGen Biotechnologies), anti–Lamin B1 mAb (L-5; Zymed Laboratories), anti–cytochrome *c* mAb (7H8.2C12; BD Biosciences), anti–glyceraldehyde-3-phosphate dehydrogenase mAb (6G7; Biogenesis), anti–caspase-3 mAb (19; Transduction), anti–caspase-7 mAb (4G2; MBL International Corporation), anti–β-actin mAb (C4; CHEMICON International Inc.), anti–Bcl-2 mAb (#100; BD Biosciences), Alexa 588–conjugated anti–mouse IgG antibody (Molecular Probes), FITC-conjugated anti–goat IgG antibody (Jackson ImmunoResearch Laboratories), gold-conjugated anti–goat IgG antibody (British BioCell), and HRP-conjugated anti–mouse IgG antibody (Cell Signaling). Anti–presenilin-1 polyclonal antibody was raised by immunizing rabbits with a synthetic peptide corresponding to residues 1–14 of human presenilin-1, and was affinity purified using ProtOn Kit1 (MultiplePeptide Systems). The chemical reagents used in this experiment were tunicamycin, thapsigargin, etoposide, staurosporine (Sigma-Aldrich), and ER-tracker and Mitotracker (Molecular Probes). Cytotoxic peptides, $A\beta_{25\text{-}35}$ and $A\beta_{1\text{-}40}$, and their reverse peptides, $A\beta_{35\text{-}25}$ and $A\beta_{40\text{-}1}$, were purchased from Sigma-Aldrich.

Cell culture

Human neuroblastoma SK-N-SH cells and human carcinoma HeLa cells were respectively cultured in α-MEM (Invitrogen) and DME (Invitrogen) both containing 10% FBS, at 37°C under 5% CO_2. For some experiments, these cells were stably transfected with pCAGGS-hBcl-2 (Iwahashi et al., 1997) and pCAGGS-hBcl-x_L (Tagami et al., 2000) to overexpress Bcl-2 and Bcl-x_L, respectively.

cDNA cloning

A human colon cDNA library (Stratagene) was used for hybridization to isolated cDNA homologous to the partial sequence of mouse caspase-12 gene.

Immunofluorescence microscopy

SK-N-SH cells or HeLa cells were incubated with or without Mitotracker probes, and were fixed with 0.1 M phosphate buffer containing 4% PFA for 2 h at 4°C. Cells were incubated with anti–caspase-4 pAb with or without anti-KDEL mAb, followed by FITC- and Alexa 588–conjugated secondary antibodies, respectively. Stained cells were observed under a confocal microscope (model LSM510; Carl Zeiss MicroImaging, Inc.). To determine localization of caspase-4 in live cells, HeLa cells were transfected with caspase-4/GFP fusion gene subcloned into a pcDNA3.1 (Invitrogen) to produce caspase-4 fused with GFP at its COOH terminus, and after 24 h, cells were incubated with ER-tracker probe for 30 min, followed by observation under a fluorescence microscope (model IX71; Olympus).

Immuno-EM

Immuno-EM was performed essentially as described previously (Miyake et al., 2002). In brief, SK-N-SH cells cultured on a 15-cm dish were fixed with 4% PFA in PBS, pH 7.2, at RT for several hours. After harvesting the cells, they were washed with 30 mM Hepes buffer, pH 7.4, several times. The cells were resuspended in 10% gelatin in 30 mM Hepes buffer, pH 7.4, at 37°C. After centrifugation to recover cells, gelatin was solidified on ice. Blocks for ultracryotomy were prepared and infused with 20% polyvinylpyrrolidone/1.84 M sucrose overnight at 4°C. Ultrathin sections were collected on nickel grids and immunostained with anti–caspase-4 pAb. The sections were incubated with gold-conjugated anti–goat IgG antibody (gold particles, 10-nm diam) for 1 h at RT. Grids were contracted in 2% uranyl acetate and examined on a transmission electron microscope (model CM10; Philips).

Subcellular fractionation

SK-N-SH cells cultured on a 15-cm dish were washed twice with PBS, harvested, and suspended in buffer A (50 mM Tris-HCl, pH 8.0, 1 mM EDTA, 0.32 M sucrose, 0.1 mM PMSF) for 5 min on ice. Then the cells were passed through a 25-gauge needle 13 times and centrifuged at 500 *g* for 10 min to collect a crude nuclear pellet. The supernatant was centrifuged at 1,200 *g* for 10 min to yield a mitochondria-enriched pellet, which contained mitochondria and microsome as shown in Fig. 1 s. This supernatant was further centrifuged at 100,000 *g* for 60 min to yield a microsomal pellet and a cytosolic fraction. All of the pellets were dissolved in buffer A containing 1% SDS. Equal volume of each fraction was subjected to Western blotting as described below, using indicated antibodies.

Western blot analysis

Cells treated with the indicated reagents were washed with PBS, harvested, and lysed in TNE buffer (10 mM Tris-HCl, pH 7.8, 1 mM EDTA, 150 mM NaCl, 1 mM PMSF) containing 0.5% NP-40. Equal amounts of protein were subjected to 12% SDS-PAGE and transferred to a PVDF membrane (Millipore). The membrane was blocked with 5% BSA and was incubated with each primary antibody, followed by incubation with an HRP-conjugated secondary antibody. Proteins were visualized with an ECL detection system (Amersham Biosciences).

Preparation and transfection of siRNAs

The annealed double-stranded siRNAs listed below were obtained from Dharmacon, and were used to decrease expression of caspase-4. Caspase-4 siRNA-a: 5′-AAGUGGCCUCUUCACAGUCAUdTdT-3′ (sense), 5′-AAAUGACUGUGAAGAGGCCACdTdT-3′ (antisense); caspase-4 siRNA-b: 5′-AAGAUUUCCUCACUGGUGUUUdTdT-3′ (sense), 5′-AAAAACACCAGTGAGGAAATCdTdT-3′ (antisense). For control, siRNA to GFP was used. GFP siRNA: 5′-P-GGCUACGUCCAGGAGCGCACC-3′ (sense), 5′-P-UGCGCUCCUGGACGUAGCCUU-3′ (antisense). These sequences were not significantly homologous to genes other than caspase-4 or GFP by BLAST search (NCBI). SK-N-SH cells were transfected at 50% confluence in 24-well plastic plates with 1.0 μg of each of the above siRNAs using Transmessenger transfection reagent (QIAGEN) according to the manufacturer's protocol. Transfected cells were incubated at 37°C for 60 h without changing the medium. siRNAs were introduced into HeLa cells by electroporation three times with 48-h intervals using Amaxa system according to the manufacturer's protocol. Efficiency of RNAi was measured by immunocytochemical analysis and Western blot analysis using anti–caspase-4 antibody or anti–β-actin antibody.

Cell viability assay

SK-N-SH cells or HeLa cells overexpressing Bcl-2 and Bcl-x_L, or transfected with siRNAs as above were treated with various reagents as indicated. When using $A\beta_{1\text{-}40}$, it was preincubated for 1 wk at 37°C to establish its cytotoxicity. Cell death was assessed on the basis of cellular morpho-

logical changes observed by phase-contrast microscopy or from nuclear morphological changes detected by fluorescence microscopy after staining the cells with 10 μM Hoechst 33342. At least 500 cells were counted, and the data was expressed as the mean ± SEM from three independent experiments and P values were calculated by *t* test. The MTS ([3-(4, 5-dimethylthiazol-2-yl)-5-(3-carboxymethoxyphenyl)-2-(4-sulfophenyl)-2H-tetrazolium, inner salt]) assay was also performed to evaluate cell viability. After treatment with apoptosis-inducing reagents, cells were coincubated with MTS solution (Promega) for 1 h at 37°C. The amount of reduced MTS released from the viable cells was quantified by measuring the absorbance at 490 nm using a spectrophotometer. Results were expressed as a ratio (%) of dead cells after treatments to those in control as above.

The authors greatly thank Ms. A. Arakawa and Ms. M. Matsumoto-Yatera for their technical assistance. We are grateful to Drs. J. Yuan, H. Ichijo, H. Nishitoh, S. Miyake, and M. Takeda for critical reading of the manuscript and for valuable advice and encouragement.

Submitted: 3 October 2003
Accepted: 6 April 2004

References

Alnemri, E.S., D.J. Livingston, D.W. Nicholson, G. Salvesen, N.A. Thornberry, W.W. Wong, and J. Yuan. 1996. Human ICE/CED-3 protease nomenclature. *Cell.* 87:171.

Bonifacino, J.S., and A.M. Weissman. 1998. Ubiquitin and the control of protein fate in the secretory and endocytic pathways. *Annu. Rev. Cell Dev. Biol.* 14: 19–57.

Brewer, J.W., J.L. Cleveland, and L.M. Hendershot. 1997. A pathway distinct from the mammalian unfolded protein response regulates expression of endoplasmic reticulum chaperones in non-stressed cells. *EMBO J.* 16:7207–7216.

Distelhorst, C.W., M. Lam, and T.S. McCormick. 1996. Bcl-2 inhibits hydrogen peroxide-induced ER Ca^{2-} pool depletion. *Oncogene.* 12:2051–2055.

Fernandes-Alnemri, T., R.C. Armstrong, J. Krebs, S.M. Srinivasula, L. Wang, F. Bullrich, L.C. Fritz, J.A. Trapani, K.J. Tomaselli, G. Litwack, and E.S. Alnemri. 1996. In vitro activation of CPP32 and Mch3 by Mch4, a novel human apoptotic cysteine protease containing two FADD-like domains. *Proc. Natl. Acad. Sci. USA.* 93:7464–7469.

Ferri, K.F., and G. Kroemer. 2001. Organelle-specific initiation of cell death pathways. *Nat. Cell Biol.* 3:E255–E263.

Fischer, H., U. Koenig, L. Eckhart, and E. Tschachler. 2002. Human caspase 12 has acquired deleterious mutations. *Biochem. Biophys. Res. Commun.* 293: 722–772.

Forman, M.S., V.M. Lee, and J.Q. Trojanowski. 2003. 'Unfolding' pathways in neurodegenerative disease. *Trends Neurosci.* 26:407–410.

Foyouzi-Youssefi, R., S. Arnaudeau, C. Borner, W.L. Kelley, J. Tschopp, D.P. Lew, N. Demaurex, and K.H. Krause. 2000. Bcl-2 decreases the free Ca^{2+} concentration within the endoplasmic reticulum. *Proc. Natl. Acad. Sci. USA.* 97:5723–5728.

Harding, H.P., Y. Zhang, and D. Ron. 1999. Protein translation and folding are coupled by an endoplasmic-reticulum-resident kinase. *Nature.* 397:271–274.

Haviv, R., L. Lindenboim, J. Yuan, and R. Stein. 1998. Need for caspase-2 in apoptosis of growth-factor-deprived PC12 cells. *J. Neurosci. Res.* 52:491–497.

He, H., M. Lam, T.S. McCormick, and C.W. Distelhorst. 1997. Maintenance of calcium homeostasis in the endoplasmic reticulum by Bcl-2. *J. Cell Biol.* 138:1219–1228.

Imai, Y., M. Soda, and R. Takahashi. 2000. Parkin suppresses unfolded protein stress-induced cell death through its E3 ubiquitin-protein ligase activity. *J. Biol. Chem.* 275:35661–35664.

Imai, Y., M. Soda, H. Inoue, N. Hattori, Y. Mizuno, and R. Takahashi. 2001. An unfolded putative transmembrane polypeptide, which can lead to endoplasmic reticulum stress, is a substrate of Parkin. *Cell.* 105:891–902.

Imaizumi, K., K. Miyoshi, T. Katayama, T. Yoneda, M. Taniguchi, T. Kudo, and M. Tohyama. 2001. The unfolded protein response and Alzheimer's disease. *Biochim. Biophys. Acta.* 1536:85–96.

Iwahashi, H., Y. Eguchi, N. Yasuhara, T. Hanafusa, Y. Matsuzawa, and Y. Tsujimoto. 1997. Synergistic anti-apoptotic activity between Bcl-2 and SMN implicated in spinal muscular atrophy. *Nature.* 390:413–417.

Kamens, J., M. Paskind, M. Hugunin, R.V. Talanian, H. Allen, D. Banach, N. Bump, M. Hackett, C.G. Johnston, P. Li, et al. 1995. Identification and characterization of ICH-2, a novel member of the interleukin-1 beta-converting enzyme family of cysteine proteases. *J. Biol. Chem.* 270:15250–15256.

Katayama, T., K. Imaizumi, N. Sato, K. Miyoshi, T. Kudo, J. Hitomi, T. Morihara, T. Yoneda, F. Gomi, Y. Mori, et al. 1999. Presenilin-1 mutations downregulate the signaling pathway of the unfolded-protein response. *Nat. Cell Biol.* 1:479–485.

Kaufman, R.J. 2002. Orchestrating the unfolded protein response in health and disease. *J. Clin. Invest.* 110:1389–1398.

Kluck, R.M., E. Bossy-Wetzel, D.R. Green, and D.D. Newmeyer. 1997. The release of cytochrome *c* from mitochondria: a primary site for Bcl-2 regulation of apoptosis. *Science.* 275:1132–1136.

Kozutsumi, Y., M. Segal, K. Normington, M.J. Gething, and J. Sambrook. 1988. The presence of malfolded proteins in the endoplasmic reticulum signals the induction of glucose-regulated proteins. *Nature.* 332:462–464.

Li, P., D. Nijhawan, I. Budihardjo, S.M. Srinivasula, M. Ahmad, E.S. Alnemri, and X. Wang. 1997. Cytochrome *c* and dATP-dependent formation of Apaf-1/caspase-9 complex initiates an apoptotic protease cascade. *Cell.* 91: 479–489.

Lin, X.Y., M.S. Choi, and A.G. Porter. 2000. Expression analysis of the human caspase-1 subfamily reveals specific regulation of the CASP5 gene by lipopolysaccharide and interferon-gamma. *J. Biol. Chem.* 275:39920–39926.

Martinon, F., K. Burns, and J. Tschopp. 2002. The inflammasome: a molecular platform triggering activation of inflammatory caspases and processing of proIL-beta. *Mol. Cell.* 10:417–426.

Miyake, S., T. Yamashita, M. Taniguchi, M. Tamatani, K. Sato, and M. Tohyama. 2002. Identification and characterization of a novel mitochondrial tricarboxylate carrier. *Biochem. Biophys. Res. Commun.* 295:463–468.

Muzio, M., A.M. Chinnaiyan, F.C. Kischkel, K. O'Rourke, A. Shevchenko, J. Ni, C. Scaffidi, J.D. Bretz, M. Zhang, R. Gentz, et al. 1996. FLICE, a novel FADD-homologous ICE/CED-3-like protease, is recruited to the CD95 (Fas/APO-1) death-inducing signaling complex. *Cell.* 85:817–827.

Nakagawa, T., and J. Yuan. 2000. Cross-talk between two cysteine protease families. Activation of caspase-12 by calpain in apoptosis. *J. Cell Biol.* 150:887–894.

Nakagawa, T., H. Zhu, N. Morishima, E. Li, J. Xu, B.A. Yankner, and J. Yuan. 2000. Caspase-12 mediates endoplasmic-reticulum-specific apoptosis and cytotoxicity by amyloid-beta. *Nature.* 403:98–103.

Nishitoh, H., A. Matsuzawa, K. Tobiume, K. Saegusa, K. Takeda, K. Inoue, S. Hori, A. Kakizuka, and H. Ichijo. 2002. ASK1 is essential for endoplasmic reticulum stress-induced neuronal cell death triggered by expanded polyglutamine repeats. *Genes Dev.* 16:1345–1355.

Oyadomari, S., E. Araki, and M. Mori. 2002. Endoplasmic reticulum stress-mediated apoptosis in pancreatic beta-cells. *Apoptosis.* 7:335–345.

Pinton, P., D. Ferrari, P. Magalhaes, K. Schulze-Osthoff, F. Di Virgilio, T. Pozzan, and R. Rizzuto. 2000. Reduced loading of intracellular $Ca^{(2+)}$ stores and downregulation of capacitative $Ca^{(2+)}$ influx in Bcl-2–overexpressing cells. *J. Cell Biol.* 148:857–862.

Rao, R.V., E. Hermel, S. Castro-Obregon, G. del Rio, L.M. Ellerby, H.M. Ellerby, and D.E. Bredesen. 2001. Coupling endoplasmic reticulum stress to the cell death program. Mechanism of caspase activation. *J. Biol. Chem.* 276:33869–33874.

Salvesen, G.S., and V.M. Dixit. 1997. Caspases: intracellular signaling by proteolysis. *Cell.* 91:443–446.

Sato, N., K. Imaizumi, T. Manabe, M. Taniguchi, J. Hitomi, T. Katayama, T. Yoneda, T. Morihara, Y. Yasuda, T. Takagi, et al. 2001. Increased production of beta-amyloid and vulnerability to endoplasmic reticulum stress by an aberrant spliced form of presenilin 2. *J. Biol. Chem.* 276:2108–2114.

Scaffidi, C., S. Fulda, A. Srinivasan, C. Friesen, F. Li, K.J. Tomaselli, K.M. Debatin, P.H. Krammer, and M.E. Peter. 1998. Two CD95 (APO-1/Fas) signaling pathways. *EMBO J.* 17:1675–1687.

Scorrano, L., S.A. Oakes, J.T. Opferman, E.H. Cheng, M.D. Sorcinelli, T. Pozzan, and S.J. Korsmeyer. 2003. BAX and BAK regulation of endoplasmic reticulum Ca^{2+}: a control point for apoptosis. *Science.* 300:135–139.

Selkoe, D.J. 1986. Altered structural proteins in plaques and tangles: what do they tell us about the biology of Alzheimer's disease? *Neurobiol. Aging.* 7:425–432.

Tagami, S., Y. Eguchi, M. Kinoshita, M. Takeda, and Y. Tsujimoto. 2000. A novel protein, RTN-XS, interacts with both Bcl-XL and Bcl-2 on endoplasmic reticulum and reduces their anti-apoptotic activity. *Oncogene.* 19:5736–5746.

Tamatani, M., T. Matsuyama, A. Yamaguchi, N. Mitsuda, Y. Tsukamoto, M. Taniguchi, Y.H. Che, K. Ozawa, O. Hori, H. Nishimura, et al. 2001. ORP150 protects against hypoxia/ischemia-induced neuronal death. *Nat. Med.* 7:317–323.

Thornberry, N.A., and Y. Lazebnik. 1998. Caspases: enemies within. *Science.* 281: 1312–1316.

Travers, K.J., C.K. Patil, L. Wodicka, D.J. Lockhart, J.S. Weissman, and P. Walter. 2000. Functional and genomic analyses reveal an essential coordina-

tion between the unfolded protein response and ER-associated degradation. *Cell.* 101:249–258.

Troy, C.M., S.A. Rabacchi, W.J. Friedman, T.F. Frappier, K. Brown, and M.L. Shelanski. 2000. Caspase-2 mediates neuronal cell death induced by beta-amyloid. *J. Neurosci.* 20:1386–1392.

Urano, F., X. Wang, A. Bertolotti, Y. Zhang, P. Chung, H.P. Harding, and D. Ron. 2000. Coupling of stress in the ER to activation of JNK protein kinases by transmembrane protein kinase IRE1. *Science.* 287:664–666.

Wang, S., M. Miura, Z. Jung, H. Zhu, V. Gagliardini, L. Shi, A.H. Greenberg, and J. Yuan. 1996. Identification and characterization of Ich-3, a member of the interleukin-1beta converting enzyme (ICE)/Ced-3 family and an upstream regulator of ICE. *J. Biol. Chem.* 271:20580–20587.

Wang, S., M. Miura, Y.K. Jung, H. Zhu, E. Li, and J. Yuan. 1998. Murine caspase-11, an ICE-interacting protease, is essential for the activation of ICE. *Cell.* 92:501–509.

Wigley, W.C., R.P. Fabunmi, M.G. Lee, C.R. Marino, S. Muallem, G.N. DeMartino, and P.J. Thomas. 1999. Dynamic association of proteasomal machinery with the centrosome. *J. Cell Biol.* 145:481–490.

Yang, J., X. Liu, K. Bhalla, C.N. Kim, A.M. Ibrado, J. Cai, T.I. Peng, D.P. Jones, and X. Wang. 1997. Prevention of apoptosis by Bcl-2: release of cytochrome *c* from mitochondria blocked. *Science.* 275:1129–1132.

Yankner, B.A., L.R. Dawes, S. Fisher, L. Villa-Komaroff, M.L. Oster-Granite, and R.L. Neve. 1989. Neurotoxicity of a fragment of the amyloid precursor associated with Alzheimer's disease. *Science.* 245:417–420.

Yoneda, T., K. Imaizumi, K. Oono, D. Yui, F. Gomi, T. Katayama, and M. Tohyama. 2001. Activation of caspase-12, an endoplastic reticulum (ER) resident caspase, through tumor necrosis factor receptor-associated factor 2-dependent mechanism in response to the ER stress. *J. Biol. Chem.* 276:13935–13940.

Zinszner, H., M. Kuroda, X. Wang, N. Batchvarova, R.T. Lightfoot, H. Remotti, J.L. Stevens, and D. Ron. 1998. CHOP is implicated in programmed cell death in response to impaired function of the endoplasmic reticulum. *Genes Dev.* 12:982–995.

Zong, W.X., C. Li, G. Hatzivassiliou, T. Lindsten, Q.C. Yu, J. Yuan, and C.B. Thompson. 2003. Bax and Bak can localize to the endoplasmic reticulum to initiate apoptosis. *J. Cell Biol.* 162:59–69.

Zou, H., W.J. Henzel, X. Liu, A. Lutschg, and X. Wang. 1997. Apaf-1, a human protein homologous to *C. elegans* CED-4, participates in cytochrome *c*-dependent activation of caspase-3. *Cell.* 90:405–413.

THE JOURNAL OF BIOLOGICAL CHEMISTRY
Vol. 279, No. 32, Issue of August 6, pp. 33865–33874, 2004
Printed in U.S.A.

A Caspase-8-independent Signaling Pathway Activated by Fas Ligation Leads to Exposure of the Bak N Terminus*

Received for publication, March 30, 2004, and in revised form, May 11, 2004
Published, JBC Papers in Press, May 24, 2004, DOI 10.1074/jbc.M403499200

Lilin Zhang‡, Shigeomi Shimizu‡, Kazuhiro Sakamaki§, Shin Yonehara§, and Yoshihide Tsujimoto‡¶

From the ‡Laboratory of Molecular Genetics, Department of Post-Genomics and Diseases, Osaka University Medical School and Solution-Oriented Research for Science and Technology, Japan Science and Technology Corp., 2-2 Yamadaoka, Suita, Osaka 565-0871 and the §Graduate School of Biostudies and Institute for Virus Research, Kyoto University, Kawahara-cho, Shogoin, Sakyo-ku, Kyoto 606-8507, Japan

Bak is a pro-apoptotic member of the Bcl-2 family that is activated by apoptotic stimulation: its activation is characterized by conformational changes such as exposure of the N terminus and oligomerization. In death receptor-mediated apoptosis, the activation of Bak depends on activation of caspase-8. However, we found that exposure of the N terminus of Bak (but not oligomerization) can occur in the absence of active caspase-8. Although exposure of the N terminus of Bak without oligomerization is not sufficient to release cytochrome *c* from the mitochondria and commit cells to apoptosis, this change sensitizes the mitochondria to apoptotic signals (including Bid) and thus sensitizes cells to apoptotic death. Fas-induced, caspase-8-independent exposure of the N terminus of Bak is blocked by staurosporine, a pan protein kinase inhibitor. These results suggest that Fas stimulation not only activates caspase-8, but also a distinct signaling pathway involving protein kinase(s) to induce exposure of the N terminus of Bak.

Mitochondria play a crucial role in many physiological and pathological cell death paradigms in mammals. Most apoptotic stimuli convey death signals to the mitochondria. During apoptosis, the permeability of the outer mitochondrial membrane increases, resulting in the release of proteins into the cytoplasm from the intermembrane space, including several apoptogenic molecules such as cytochrome *c*, Smac (Diablo), HtrA2 (Omi), and apoptosis-inducing factor. After being released into the cytoplasm, cytochrome *c* binds to apoptotic protease activating factor 1, which recruits and activates procaspase-9, triggering the activation of the caspase cascade and committing the cell to apoptotic death. Smac (Diablo) and HtrA2 (Omi) facilitate caspase activation by inhibiting inhibitor of apoptosis proteins, which are endogenous caspase inhibitors (1, 2). Mitochondrial membrane permeability is regulated by a group of proteins called the Bcl-2 family. This family of proteins can be divided into anti-apoptotic members (Bcl-2, Bcl-x_L, and Mcl-1) and pro-apoptotic members, which consist of multidomain members (Bak and Bax) and BH3-only proteins (Bid, Bim, Bik, Bad, Noxa, and Puma) (3, 4). Multidomain pro-apoptotic Bak and Bax are functionally redundant and play a direct role in increasing mitochondrial membrane permeability, leading to the release of apoptogenic proteins (5, 6). BH3-only proteins are thought to function as death signal sensors. After apoptotic stimulation, these proteins are primarily activated by different mechanism(s) and then activate Bak/Bax by still unknown mechanism(s) or inactivate anti-apoptotic Bcl-2 family members, finally leading to an increase of mitochondrial membrane permeability (3, 4).

Engagement of death receptors such as Fas and tumor necrosis factor α (TNFα)[1] receptor leads to one of two distinct apoptotic signaling pathways, which mainly differ in the extent of caspase-8 activation. In type I cells, there is extensive caspase-8 activation, which is sufficient to activate downstream execution caspases such as caspase-3 or caspase-7 and commit the cell to apoptotic death. In type II cells, there is less caspase-8 activation, so mitochondrial amplification of the apoptotic signal is required (7). In the latter type of cell, activated caspase-8 cleaves and activates a BH3-only protein, Bid (8, 9), which conveys apoptotic signals to the mitochondria by activating pro-apoptotic Bax or Bak (10–12). Because Bax and Bak are constitutively expressed, and the amount of these proteins usually remains unchanged during apoptosis, it is believed that Bak or Bax activation is regulated at the post-translational level (3, 13, 14). Bax is localized in the cytoplasm of living cells: after apoptotic stimulation, Bax translocates to the outer mitochondrial membrane where it oligomerizes and induces the formation of protein-conducting pores that release apoptogenic proteins (3, 12, 15–17). Bak is present on the outer mitochondrial membrane in a latent form: after accepting an upstream apoptotic signal, it undergoes oligomerization and induces the release of apoptogenic molecules from the mitochondria (11, 18).

Concealed epitopes at the N terminus of Bax or Bak are revealed after apoptotic stimulation, suggesting that a conformational change occurs in Bax and Bak or that a binding protein (which masks the N terminus) undergoes dissociation

* This work was supported by a grant for Scientific Research on Priority Areas, a grant for Center of Excellence Research, a grant for Scientific Research from the Ministry of Education, Science, Sports, and Culture of Japan, and by Special Coordination Funds for Promoting Science and Technology from the Science and Technology Agency of Japan. The costs of publication of this article were defrayed in part by the payment of page charges. This article must therefore be hereby marked "*advertisement*" in accordance with 18 U.S.C. Section 1734 solely to indicate this fact.

¶ To whom correspondence should be addressed. Tel.: 81-6-6879-3363; Fax: 81-6-6879-3369; E-mail: tsujimot@gene.med.osaka-u.ac.jp.

[1] The abbreviations used are: TNF, tumor necrosis factor; DSS, disuccinimidyl suberate; BMH, bismaleimidohexane; FBS, fetal bovine serum; MEF, mouse embryonic fibroblast; PBS, phosphate-buffered saline; CHAPS, 3-[(3-cholamidopropyl)dimethylammonio]-1-propanesulfonic acid; siRNA, small interference RNA; GFP, green fluorescent protein; STS, staurosporine; z-VAD-fmk, benzyloxycarbonyl-VAD-fluoromethyl ketone; FACS, fluorescence-activated cell sorting; ERK, extracellular signal-regulated kinase; JNK, c-Jun N-terminal kinase; rBid, recombinant human Bid.

(10, 13, 14, 19). Because it has been reported that exposure of the N terminus of Bax precedes its translocation to the mitochondria and oligomerization (12, 20), it seems that exposure of the N terminus of Bax or Bak represents an intermediate step leading to their activation. Oligomerization of Bax/Bak is thought to reflect its activation, because Bax/Bak oligomerizes after apoptotic stimulation, and this process is correlated precisely with the release of cytochrome *c*, and oligomerized Bax, but not monomeric Bax, induces cytochrome *c* releasing from the isolated mitochondria (11, 12, 15, 21). However, the process of regulation of the activation of Bak during apoptosis, and the relationship between exposure of the N terminus of Bak and oligomerization in the activation process, are still unclear.

In the present study, we found that Fas stimulation elicited a caspase-8-independent signal that induced exposure of the N terminus of Bak. This N-terminal exposure was not sufficient for full activation of Bak, but primed it to become more sensitive to apoptotic signals causing full activation.

EXPERIMENTAL PROCEDURES

Antibodies and Reagents—Anti-Bak (Ab1) monoclonal antibody was purchased from Oncogene Research Products (Boston, MA). Anti-Bax (N20) and anti-Bid polyclonal antibodies were obtained from Santa Cruz Biotechnology (Santa Cruz, CA) and R&D System (Minneapolis, MN), respectively. Anti-cytochrome *c* (6H2 and 7H8) and anti-mouse-Fas (Jo2) monoclonal antibodies were from BD Pharmingen. Anti-human Fas (CH11), anti-caspase-3, and anti-caspase-8 monoclonal antibodies were obtained from MBL (Nagoya, Japan). Anti-glyceraldehyde-3-phosphate dehydrogenase and anti-porin (voltage-dependent anion channel protein) monoclonal antibodies were obtained from Chemicon (Temecula, CA) and Calbiochem (San Diego, CA), respectively. All of the secondary antibodies were purchased from Molecular Probes (Eugene, OR).

The cross-linkers disuccinimidyl suberate (DSS) and bismaleimidohexane (BMH) were from Pierce Biotechnology (Rockford, IL). Other chemicals were obtained from Sigma. Recombinant human Bid (rBid) was prepared as described previously (22).

Cell Culture—The human HeLa cell line, human Jurkat T-leukemic cell line and Jurkat caspase-8-deficient subline (JB6) (23) were grown in RPMI 1640 medium supplemented with 10% fetal bovine serum (FBS). Mouse embryonic fibroblasts (MEFs) derived from caspase-8-deficient mice were grown in Dulbecco's modified Eagle's medium supplemented with 10% FBS.

Immunofluorescence Staining—Cells were fixed in 4% paraformaldehyde for 30 min and then permeabilized with 0.1% Triton X-100 for 15 min at room temperature. After incubation with 2% FBS in phosphate-buffered saline (PBS) for 1 h, the cells were incubated with anti-Bak (Ab1) (1:500) or anti-cytochrome *c* (1:500) for 1 h. After washing three times with PBS, the cells were incubated with the secondary antibody (Alexa 488-conjugated anti-mouse IgG) for 1 h. Then fluorescence was detected under a confocal microscope (Zeiss, LSM510).

Jurkat cells were fixed, permeabilized, and blocked with 20% FBS in PBS and then incubated with anti-Bak (Ab1) antibody followed by a secondary antibody (Alexa 568-conjugated anti-mouse IgG). The cells were subsequently analyzed by a flow cytometer (BD Biosciences, FACSCalibur) or observed under a confocal fluorescence microscope. In all immunostaining experiments, normal mouse IgG was added instead of the primary antibody (IgG) as a negative control.

Analysis of Cell Death—Cell viability was detected by staining with Annexin-V or Hoechst 33342. Briefly, cells were stained with Cy3-conjugated Annexin-V or 1 μM Hoechst 33342 for 5 min at room temperature and then analyzed using a flow cytometer or examined under a fluorescence microscope (Olympus, BX50).

Gel Filtration Analysis—Jurkat cells were treated, harvested, and extracted with HNC buffer (25 mM HEPES (pH7.5), 300 mM NaCl, 1 mM dithiothreitol, 2% CHAPS). The extracts were applied to a Superdex 200 HR 10/30 column (Amersham Biosciences), and fractions (40 μl) were collected for analysis by Western blotting. In some experiments, extracts were incubated with anti-Bak (Ab1) antibody or normal mouse IgG for 3 h before being applied to the column.

Cross-linking—Jurkat cells were harvested, incubated with 1 mM or 0.1 mM BMH for 30 min at room temperature, and then incubated with 1 mM dithiothreitol for 15 min to quench the cross-linker. Next, the cells were solubilized in sample buffer and analyzed by Western blotting. When the cross-linker DSS was used, Jurkat cells were lysed with HNC buffer, and then the lysates were incubated with 1 mM DSS for 30 min at room temperature, followed by incubation with 100 mM Tris buffer (pH 7.4) for 15 min to quench the cross-linker. As a control, the same concentration of Me_2SO was added instead of reagents.

siRNA Study—All siRNAs were produced by Dharmacon Research, and their sequences were as follows (numbers in parentheses indicate nucleotide positions within the respective open reading frame): mouse Bak (65–85), 5′-AACAGCAGGUUGCCCAGGACA-3′; mouse Bax (231–252), 5′-AGGAUGAUUGCUGACGUGGAC-3′; and GFP (274–294), 5′-GGCUACGUCCAGGAGCGCACC-3′. Cells were transfected with siRNA by electroporation using an Amaxa System three times at 48-h intervals.

Permeabilized Cells—HeLa cells were cultured in 10-well glass slides. After washing twice with isotonic buffer (20 mM Hepes-KOH (pH 7.4), 1.5 mM $MgCl_2$, 10 mM KCl, 250 mM sucrose), the cells were incubated with isotonic buffer containing 20 μg/ml digitonin for 3 min at room temperature. After washing three times with isotonic buffer, the cells were incubated with cytosol or rBid for 10 min at 37 °C. After washing another three times with isotonic buffer, the cells were subjected to immunostaining.

Preparation of Cytosol—After washing three times with isotonic buffer, cells were suspended in the same volume of isotonic buffer supplemented with protease inhibitors, and then homogenized using a Dounce homogenizer. After centrifugation at 100,000 × *g* for 1 h, the supernatant was obtained and used as the cytosol.

Subcellular Fractionation—Cells were fractionated as described previously (24). Briefly, cells were harvested, washed three times with isotonic buffer, and then incubated with 30 μg/ml digitonin in isotonic buffer for 5 min at 37 °C. After centrifugation at 3000 rpm for 3 min, aliquots of the supernatant (cytosolic fractions) and the pellet (containing the mitochondria) were analyzed by Western blotting with an anti-cytochrome *c* antibody.

In Vitro Analysis of Cytochrome c Release—Mitochondria were prepared from the livers of male Donryu rats as described previously (25). Briefly, the livers were harvested and homogenized in buffer A (0.3 M mannitol, 10 mM potassium Hepes (pH 7.4), 0.1% fatty acid-free bovine serum albumin, 0.2 mM EDTA) with a glass-Teflon Potter homogenizer. Then isolated mitochondria (100 μg of protein) were suspended in buffer B (buffer A plus 100 μM potassium phosphate and 4.3 mM succinate instead of EDTA) and incubated with 5 μl (40 μg of protein) of cytosol or with isotonic buffer for 5 min at room temperature, followed by incubation with or without rBid (30 μg) for a further 20 min. The mitochondria were collected by centrifugation (15,000 rpm, 5 min), and the supernatant was analyzed by Western blotting with an anti-cytochrome *c* antibody.

RESULTS

Caspase-independent Exposure of the N Terminus of Bak Occurs in Fas-stimulated Cells—Using a monoclonal antibody (anti-Bak Ab1) that recognized the N-terminal epitope of human Bak, we examined whether there were any changes to the N terminus of Bak in HeLa cells treated with an agonistic anti-Fas antibody, CH11. As reported previously (13, 19), Bak could not be recognized in living cells by Ab1 antibody, whereas cells exhibited increased immunoreactivity to Ab1 antibody after Fas stimulation (Fig. 1, *A* and *B*). Because we could not detect any change of Bak protein content after treatment with CH11 (Fig. 1*C*), this increased immunoreactivity to Ab1 antibody indicated exposure of the N terminus of Bak. Exposure of the N terminus could be detected after 1 h of treatment with CH11, when only a few cells had died (Fig. 1, *B* and *D*), consistent with the findings of others that exposure of the N terminus was an early event occurring before morphological changes (13, 19).

In HeLa cells (type II cells), Fas stimulation initiates the activation of caspase-8, which cleaves Bid, a pro-apoptotic member of the Bcl-2 family, and truncated Bid translocates to the mitochondria and activates Bak or Bax by a still unidentified mechanism (9–11). To investigate whether caspase-8 is involved in exposure of the N terminus of Bak, we employed a broad spectrum caspase inhibitor (z-VAD-fmk) to suppress caspase activation. Unexpectedly, we found that z-VAD-fmk (100 μM) did not affect the increased immunoreactivity to Ab1

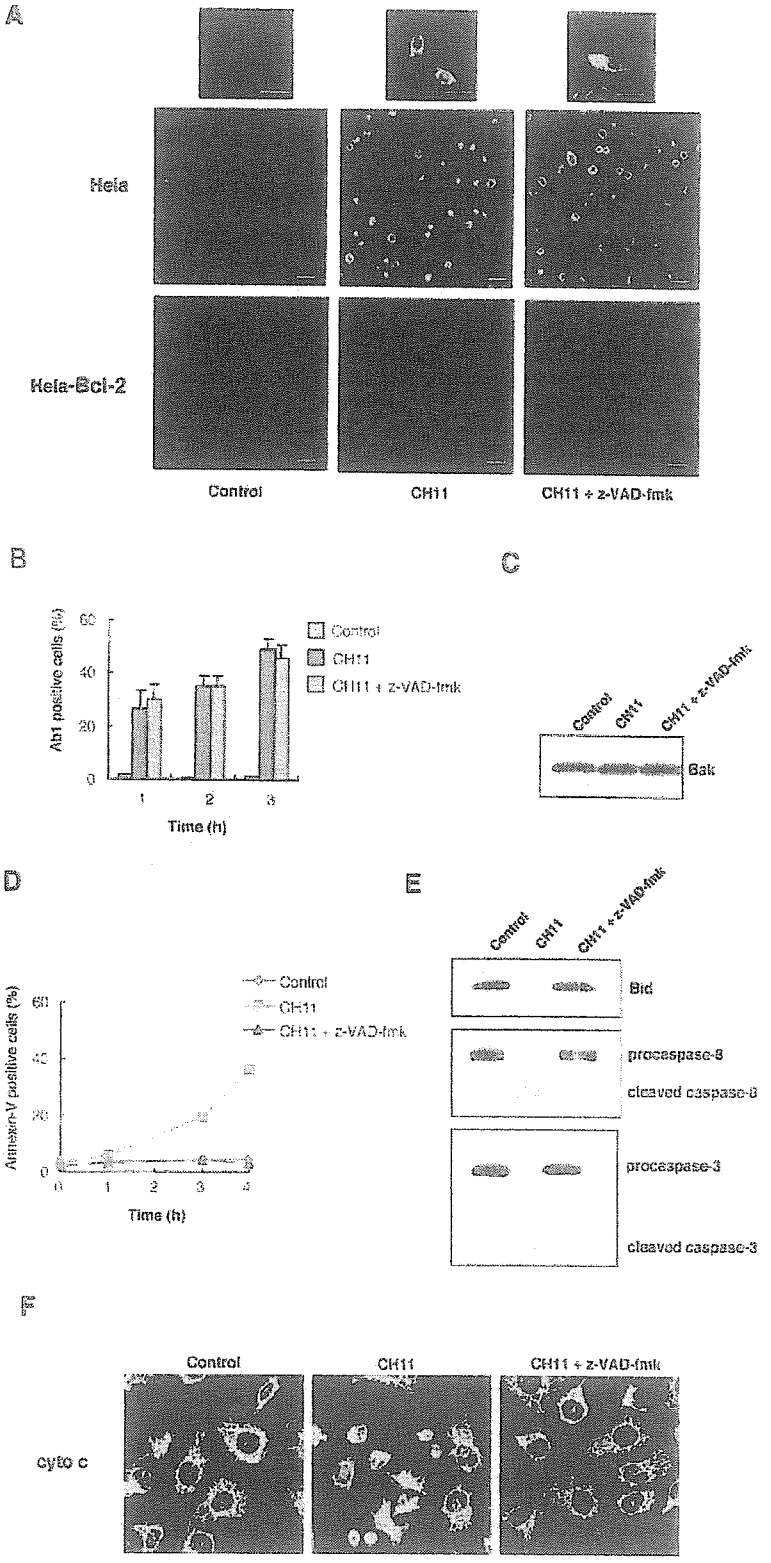

FIG. 1. **CH11-induced exposure of the N terminus of Bak in the presence of z-VAD-fmk.** *A* and *B*, HeLa cells and HeLa cells overexpressing Bcl-2 (HeLa-Bcl-2) were treated without or with CH11 (0.5 μg/ml) for 4 h (*A*) or for the indicated times (*B*) in the presence or absence of z-VAD-fmk (100 μM). Cells were immunostained with a monoclonal anti-Bak Ab1 antibody. *A*, representative images are shown. *Scale bar* = 20 μm. *Top*: enlarged images of immunostaining. *B*, Ab1-positive cells from four randomly chosen fields were counted under a confocal microscope. Data are shown as the mean ± S.E. (n = 3). *C*, Western blot analysis of Bak from HeLa cells treated as indicated for 4 h. *D*, inhibition of CH11-induced apoptosis of HeLa cells by z-VAD-fmk. *E*, inhibition by z-VAD-fmk of cleavage of Bid and the activation of caspase-8 and caspase-3 in HeLa cells. HeLa cells were treated without or with CH11 (0.5 μg/ml) in the presence or absence of z-VAD-fmk (100 μM) for 8 h and then subjected to Western blot analysis with the indicated antibodies. *F*, inhibition of CH11-induced release of cytochrome *c* by z-VAD-fmk. HeLa cells were treated without or with CH11 (0.5 μg/ml) in the presence or absence of z-VAD-fmk (100 μM) for 4 h and then immunostained with a monoclonal anti-cytochrome *c* antibody.

antibody in CH11-treated cells (Fig. 1, *A* and *B*), although the dose of z-VAD-fmk that we used could almost completely suppress the activation of caspases-8, cleavage of Bid, release of cytochrome *c* from the mitochondria, activation of caspase-3, and cell death (Fig. 1, *D–F*).

Because Bcl-2/Bcl-x_L is known to inhibit the activation of Bax and Bak (26, 27), we also examined whether CH11-induced exposure of the N terminus of Bak was inhibited by Bcl-2. As shown in Fig. 1*A*, overexpression of Bcl-2 completely inhibited exposure of the N terminus of Bak in CH11-treated cells with or without exposure to z-VAD-fmk.

We next tested whether the same phenomenon also occurred

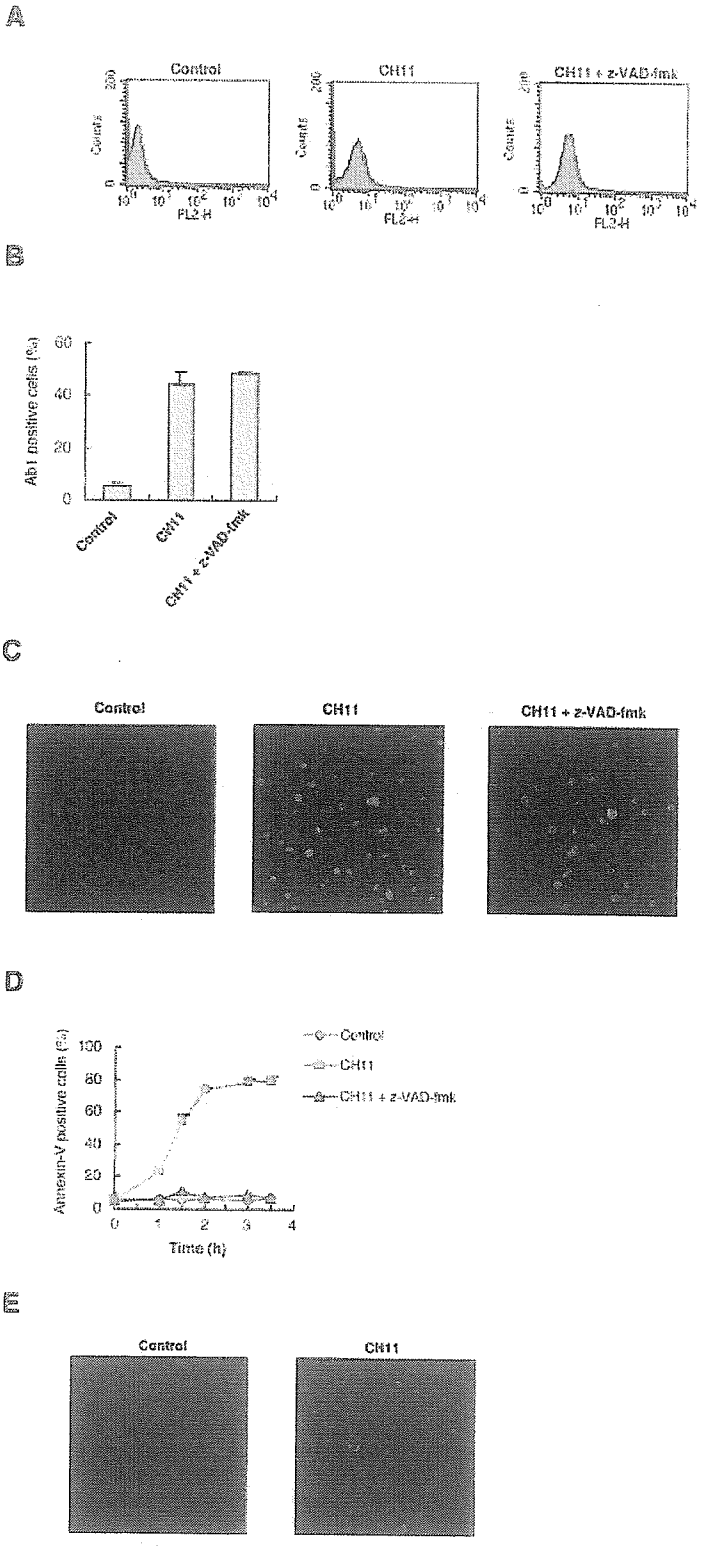

FIG. 2. **Exposure of the N terminus of Bak in Jurkat cells treated with CH11 in the presence of z-VAD-fmk.** *A–C*, Jurkat cells were treated without or with CH11 (0.5 μg/ml) for 30 min in the presence or absence of z-VAD-fmk (100 μM). Then immunostaining was performed with anti-Bak Ab1 antibody, followed by FACS analysis (*A* and *B*) or confocal microscopy examination (*C*). In *B*, Ab1-positive cells were counted by FACS analysis. Data are shown as the mean ± S.E. (n = 3). *D*, inhibition of CH11-induced apoptosis by z-VAD-fmk (100 μM). *E*, JB6 cells were treated without or with CH11 (0.5 μg/ml) for 1 h, and then immunostaining was performed with anti-Bak Ab1 antibody followed by confocal microscopy examination.

in other cell lines. As was the case for HeLa cells exposed to CH11, CH11-stimulated Jurkat cells displayed an increase of immunoreactivity to Ab1 antibody, which was not affected by z-VAD-fmk as assessed by FACS and confocal microscopy (Fig. 2, *A–C*). The dose of z-VAD-fmk used (100 μM) completely inhibited the activation of caspases, cleavage of Bid, and cell death (Fig. 2*D* and data not shown). Furthermore, we also found that exposure of the N terminus of Bak occurred in Fas-stimulated JB6 cells, a caspase-8-deficient subline of Jurkat cells (Fig. 2*E*). These results suggest that Fas stimulation could activate a caspase-8-independent signaling pathway and induce exposure of the N terminus of Bak, but this change of

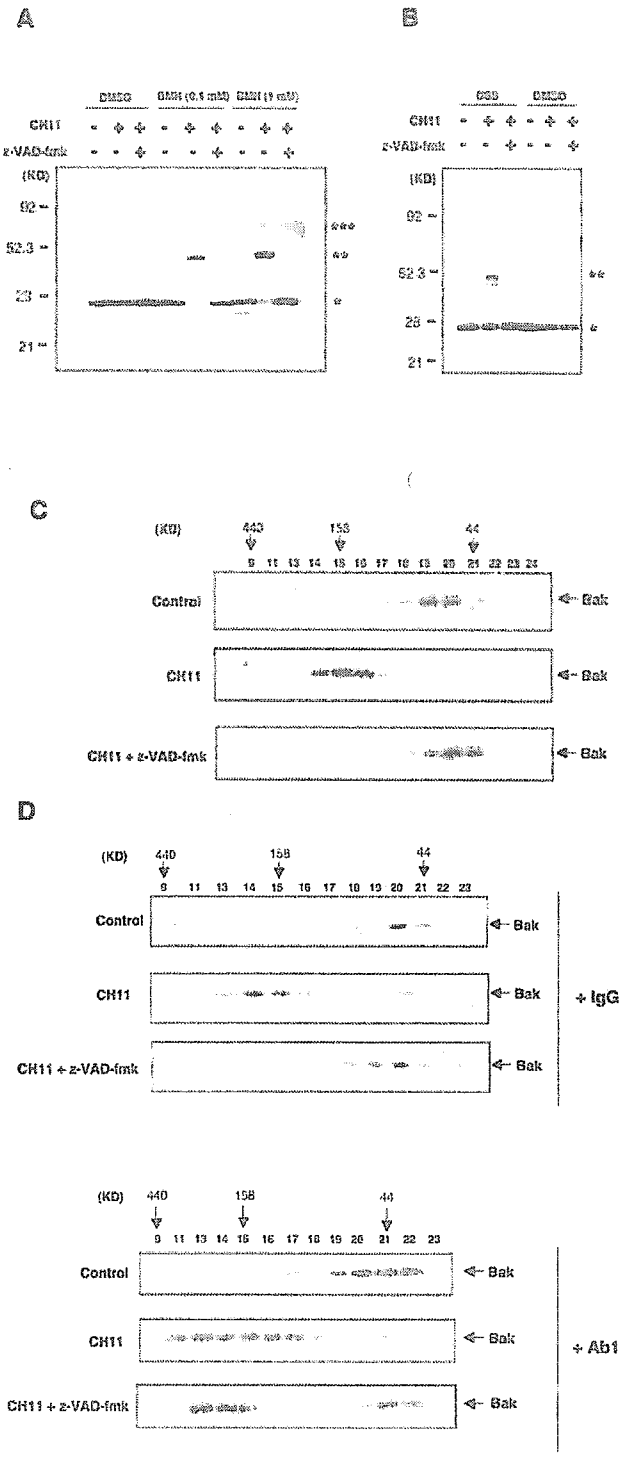

FIG. 3. **Oligomerization of Bak in Fas-stimulated Jurkat cells, and its inhibition by z-VAD-fmk.** *A*, Jurkat cells were treated without or with CH11 (0.5 μg/ml) in the presence or absence of z-VAD-fmk (100 μM) for 2 h, harvested, and incubated with a cross-linker, BMH (uncleavable), or Me_2SO (the solvent) for 30 min at room temperature. Oligomerization of Bak was detected by Western blotting. The *asterisks* denote monomeric, dimeric, trimeric Bak, respectively. *B*, Jurkat cells were treated with CH11 (0.5 μg/ml) in the presence or absence of z-VAD-fmk (100 μM) for 2 h, followed by lysis and incubation with 1 mM DSS or Me_2SO for 30 min at room temperature. Oligomerization of Bak was assayed by Western blotting. *C* and *D*, Jurkat cells were treated with CH11 (0.5 μg/ml) for 1 h in the presence or absence of z-VAD-fmk (100 μM). The lysates were incubated without (*C*) or with (*D*) anti-Bak Ab1 antibody or normal mouse IgG for 3 h and then analyzed by gel filtration column chromatography. The distribution of Bak was analyzed by Western blotting.

Bak was not sufficient for full activation.

Fas-induced Caspase-independent Exposure of the N Terminus of Bak Is Separable from Oligomerization—Previous studies indicated that Bak undergoes homo-oligomerization in apoptotic cells (11, 18, 28). Because its oligomerization is correlated with the release of cytochrome *c* from the mitochondria (11), it is thought to represent activation. Oligomerization of Bak can be detected either by using a protein cross-linker or by gel filtration column chromatography (11, 15). With these procedures, we showed that Bak was oligomerized in CH11-treated cells and this change was inhibited by z-VAD-fmk (Fig. 3, *A–C*), indicating that its oligomerization was dependent on the activation of caspases. These results suggested that caspase-independent exposure of the N terminus of Bak was separable from its oligomerization.

We further confirmed caspase-8-independent exposure of the N terminus of Bak by gel filtration. Lysates of Jurkat cells treated with or without CH11 in the presence or absence of z-VAD-fmk were incubated with Ab1 antibody or normal mouse IgG before being subjected to gel filtration column chromatography. If Bak binds to Ab1 antibody, it would be eluted in the fractions that correspond to the larger molecular size proteins. As shown in Fig. 3*D*, when the sample from untreated cells was incubated with Ab1 antibody and then applied to the column, Bak was detected in the fractions corresponding to low molecular weight proteins, as was the case without incubation with Ab1 antibody (Fig. 3*C*) or after incubation with control normal mouse IgG (Fig. 3*D*, *upper panel*), indicating no exposure of the N terminus of Bak. When the sample from CH11-treated cells was incubated with Ab1 antibody, Bak shifted to the larger molecular weight fractions, which were larger than that when the sample was incubated with normal mouse IgG or without Ab1 antibody (Fig. 3, *C* and *D*), suggesting that the N terminus was exposed in apoptotic cell lysates. When lysates from cells treated with CH11 in the presence of z-VAD-fmk were incubated with Ab1 antibody, the Bak peak was found in fractions that corresponded to both high and low molecular weight proteins (Fig. 3*D*, *lower panel*), indicating that Bak was recognized by Ab1 antibody in cells treated with CH11 in the presence of z-VAD-fmk. This result is consistent with our immunostaining data. Taken together, these observations suggest that Fas stimulation induces exposure of the N terminus of Bak in a caspase-8-independent manner and that N-terminal exposure is separable from the oligomerization of Bak.

Exposure of the N Terminus of Bak Makes Cells More Sensitive to Apoptotic Stimuli—The results described above showed that Fas-dependent/caspase-independent exposure of the N terminus of Bak did not lead to its full activation. Did such exposure of N terminus have any biological significance? We hypothesized that full activation of Bak requires at least two steps, *i.e.* exposure of the N terminus, followed by oligomerization, and that Bak with N-terminal exposure might be in a "primed state." It should be noted that exposure of the N terminus can be mediated by both caspase-8-dependent and independent mechanisms. If this hypothesis is correct, cells in which the N terminus of Bak is exposed may be more sensitive to subsequent death stimuli. To test this possibility, Jurkat cells were pretreated with CH11 in the presence of z-VAD-fmk for 2 h to "prime" Bak, and then were exposed to 10 μM VP-16 (etoposide) in the presence of z-VAD-fmk. z-VAD-fmk did not inhibit transmission of VP-16-induced death signals to the mitochondria or release of cytochrome *c* from the mitochondria

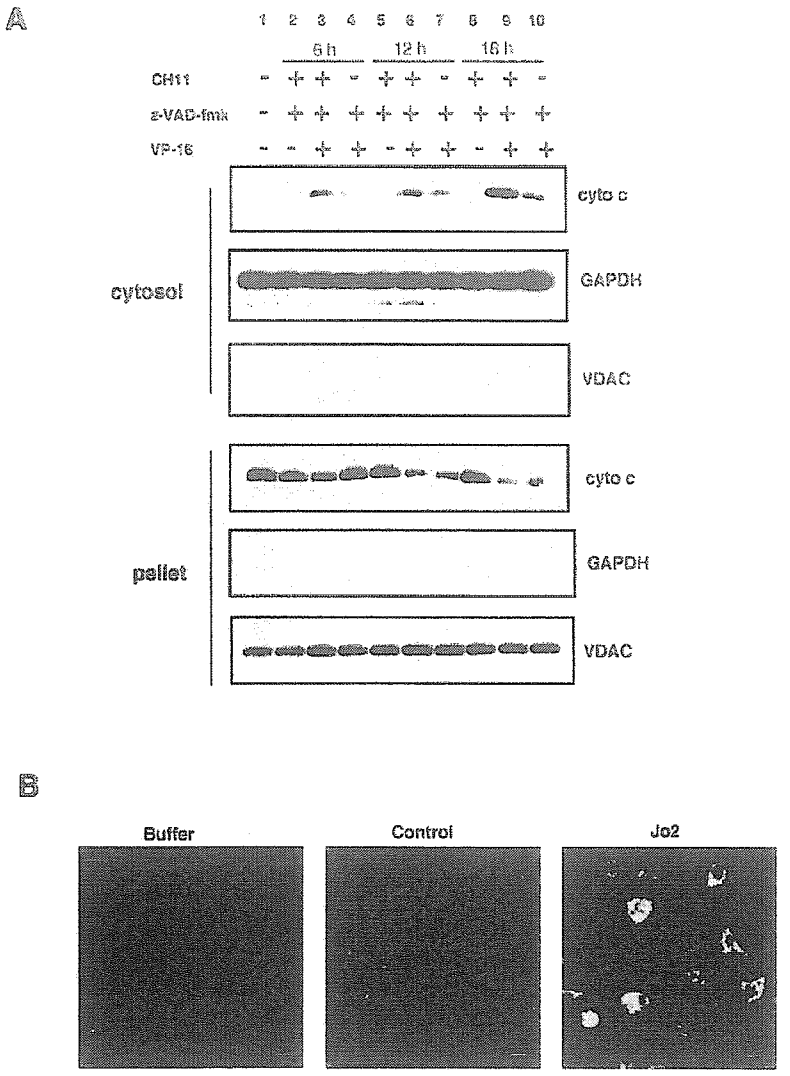

FIG. 4. **Increased susceptibility to VP-16-induced apoptosis of cells possessing Bak with N-terminal exposure.** *A*, Jurkat cells were treated with or without CH11 (0.5 μg/ml) in the presence of z-VAD-fmk (100 μM) for 2 h, followed by incubation with VP-16 (10 μM) in the presence of z-VAD-fmk for the indicated times. The cells were fractionated into cytosolic (cytosol) and organellar (pellet) fractions, and then analyzed by Western blotting with anti-cytochrome *c* antibody. Glyceraldehyde-3-phosphate dehydrogenase (*GAPDH*) and voltage-dependent anion channel protein (*VDAC*) were monitored to verify successful fractionation and as loading controls. *B*, cytosol was prepared from caspase-$8^{-/-}$ MEFs treated without (*control*) or with Jo2 (0.5 μg/ml) for 16 h and was added to HeLa cells that had been permeabilized by incubation with digitonin (20 μg/ml) for 3 min at room temperature. After incubation for 10 min at 37 °C, immunostaining was done with anti-Bak Ab1 antibody. As a negative control, isotonic buffer was added instead of cytosol. *Scale bar* = 10 μm. *C*, caspase-$8^{-/-}$ MEFs were treated with Jo2 (0.5 μg/ml) or TNFα (10 ng/ml) for 16 h, followed by incubation with 10 μM VP-16 for the indicated times. Apoptotic cells were detected by Annexin-V staining. Data are shown as the mean ± S.E. (n = 3). *D*, caspase-$8^{-/-}$ MEFs were pretreated as described in *C*, followed by incubation with 10 μM VP-16 for 24 h, and then stained with Hoechst 33342. *Scale bar* = 10 μm. *E*, caspase-$8^{-/-}$ MEFs were treated with Jo2 (0.5 μg/ml) or TNFα (10 ng/ml) for 16 h, followed by incubation with 10 μM VP-16 for 18 h. The cells were fractionated into cytosolic (cytosol) and organellar (pellet) fractions, and then extracts were subjected to Western blotting with anti-cytochrome *c* antibody. *F*, caspase-$8^{-/-}$ MEFs were treated with Jo2 (0.5 μg/ml) or TNFα (10 ng/ml) for 16 h, followed by incubation with 10 μM VP-16 for 18 h. After lysis, the activation of caspase-3 was assayed by Western blotting.

(data not shown). VP-16 induced the release of only a small amount of cytochrome *c* from the mitochondria in the cells without CH11 pretreatment (Fig. 4*A*, *lanes 4*, *7*, and *10*). In contrast, a large amount of cytochrome *c* was released after cells were pretreated with CH11/z-VAD-fmk and then exposed to VP-16 (Fig. 4*A*, *lanes 3*, *6*, and *9*). This result indicates that, although CH11 alone could not induce cytochrome *c* release in the presence of z-VAD-fmk (Fig. 4*A*, *lanes 2*, *5*, and *8*), it sensitized cells to subsequent treatment with VP-16, suggesting that Bak with N-terminal exposure might represent "primed Bak."

We also examined whether Fas-induced caspase-independent exposure of the N terminus of Bak could sensitize cells to apoptotic death. Because z-VAD-fmk inhibits apoptosis, we could not use it in experiments that assayed cell death. Therefore, we employed caspase-8-deficient murine embryonic fibroblasts (MEFs), which are completely resistant to death receptor-mediated apoptosis (29). First, we investigated whether stimulation of Fas with agonistic anti-mouse Fas antibody Jo2 induced exposure of the N terminus of Bak in caspase-8-deficient MEFs. Because no antibody was available to recognize a conformational change of mouse Bak, we employed an *in vitro* assay system using HeLa cells permeabilized by digitonin. Lysates derived from caspase-$8^{-/-}$ MEFs treated with or without Jo2 were added to digitonin-permeabilized HeLa cells, and then immunostaining was performed with Ab1 antibody. As shown in Fig. 4*B*, lysate from Jo2-treated caspase-$8^{-/-}$ MEFs, but not lysate from untreated cells, caused an increase of Ab1 immunoreactivity. This indicated that, as in Jurkat and HeLa cells, one or more factors that induced exposure of the N terminus of Bak existed in the lysates of Jo2-treated caspase-$8^{-/-}$ MEFs and, although not proved, suggested that Bak entered a primed state in caspase-$8^{-/-}$ MEFs after Jo2 treatment.

To examine whether Jo2-treated caspase-$8^{-/-}$ MEFs, in which Bak was considered to exist in a primed state, were more sensitive to death stimuli, we pretreated caspase-$8^{-/-}$ MEFs with Jo2 alone for 16 h, followed by exposure to 10 μM VP-16. Note that cycloheximide was not added here, because cycloheximide inhibited VP-16-induced apoptosis in MEFs (data not shown). As shown in Fig. 4 (*C* and *D*), pretreatment with Jo2 enhanced VP-16-induced apoptosis. The same result was also obtained with TNFα instead of Jo2 (Fig. 4, *C* and *D*). After 18 h of exposure to VP-16, Jo2- or TNFα-treated cells exhibited release of cytochrome *c* into the cytosol and activation of caspase-3, whereas untreated cells did not show any release of cytochrome *c* or caspase-3 activation at this time (Fig. 4, *E* and *F*). Consistent with a previous report (29), Jo2 or TNFα alone did not induce cytochrome *c* release (data not shown) or death of caspase-$8^{-/-}$ MEFs (Fig. 4, *C* and *D*). These results indicate

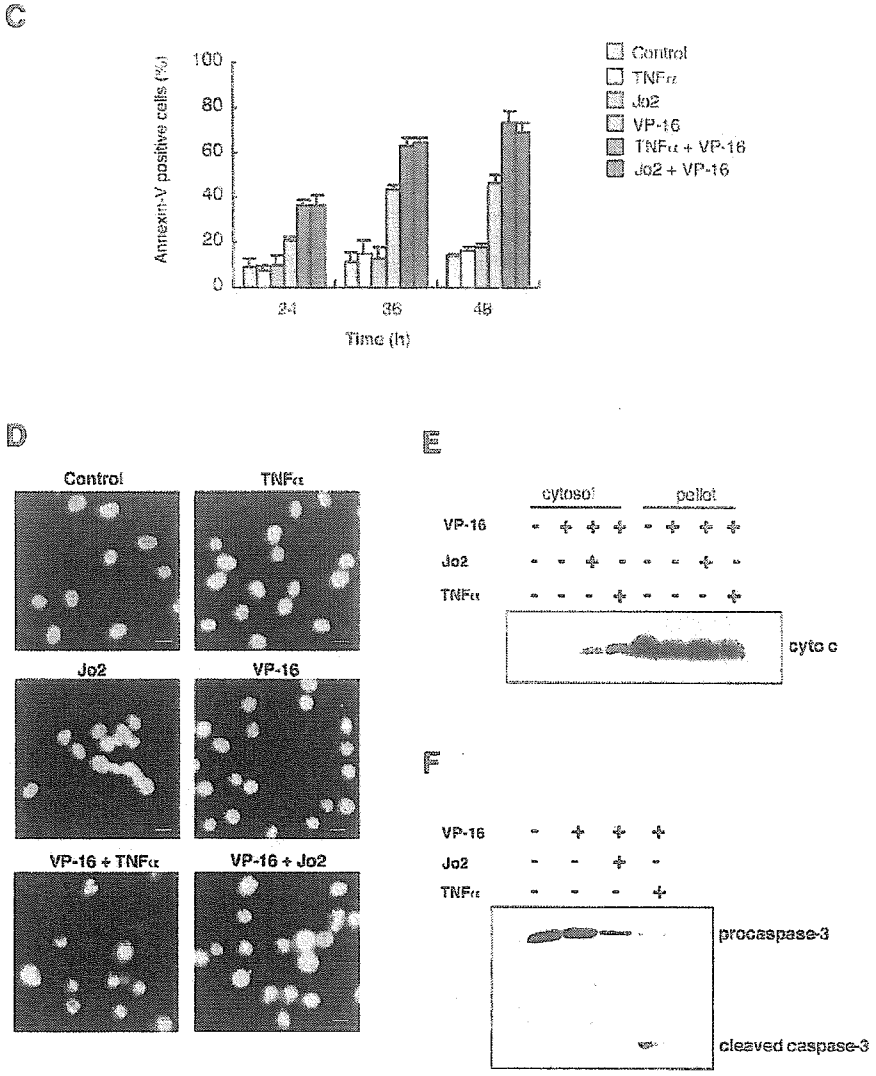

FIG. 4—*continued*

that Fas stimulation without caspase-8 activation could sensitize cells to apoptotic death.

Cytosol from Cells with Primed Bak Enhances Bid-induced Release of Cytochrome c from Isolated Mitochondria—To assess whether Fas stimulation without caspase-8 activation (leading to exposure of the N terminus of Bak) could sensitize the mitochondria to apoptotic signals, we used an *in vitro* system with mitochondria isolated from rat livers. The mitochondria were incubated for 5 min with cytosol derived from caspase-$8^{-/-}$ MEFs with or without Jo2 treatment, followed by incubation with rBid (30 μg/ml) for an additional 20 min. Release of cytochrome *c* was detected by Western blotting. As shown in Fig. 5, treatment with rBid induced the release of cytochrome *c* from isolated mitochondria, and preincubation with cytosol obtained from untreated cells only slightly promoted the release of cytochrome *c*, whereas preincubation with cytosol from treated cells markedly promoted its release. The incubation of isolated mitochondria with cytosol alone only induced slight release of cytochrome *c* (Fig. 5). These results indicate that Fas stimulation without caspase-8 activation induces a signal that could sensitize the mitochondria to apoptotic stimuli.

Bak Has an Essential Role in the Increased Susceptibility to VP-16 of Cells Possessing Bak with Caspase-8-independent N-terminal Exposure—To investigate whether the increased susceptibility to VP-16 of Jo2- or TNFα-pretreated caspase-$8^{-/-}$ MEFs was due to primed Bak, we used RNA interference to silence the expression of Bak in caspase-$8^{-/-}$ MEFs. Cells were transfected with Bak siRNA, or GFP siRNA (as a negative control), and then the expression of Bak was examined by Western blotting. As shown in Fig. 6*A*, Bak expression decreased to a nearly undetectable level after treatment with siRNA for Bak, and the silencing effect lasted for more than 72 h, whereas the Bax level remained unchanged. As observed above, Jo2- or TNFα-pretreated caspase-$8^{-/-}$ MEFs displayed an increase of susceptibility to VP-16-induced apoptosis when transfected with control GFP siRNA, whereas Jo2 or TNFα could not sensitize these cells to VP-16 after Bak was eliminated by siRNA treatment (Fig. 6*B*). It should be noted that silencing of Bak did not affect VP-16-induced apoptosis (Fig. 6*B*), which was probably mediated by Bax. In contrast, when Bax was eliminated by using Bax siRNA (Fig. 6*C*), the susceptibility of Jo2- or TNFα-pretreated caspase-$8^{-/-}$ MEFs to VP-16 was unchanged (Fig. 6*D*). Taken together, these data indicate that Bak plays an important role in the increased susceptibility to VP-16 of Jo2- or TNFα-treated cells.

A Staurosporine-sensitive Signal Elicited by Fas Ligation Is Responsible for Caspase-independent Exposure of the N Terminus of Bak—In addition to the well characterized caspase-8-de-

pendent apoptotic pathway, Fas stimulation has also been shown to activate other signaling pathways that lead to the activation of extracellular signal-regulated kinase (ERK) (30–32), c-Jun N-terminal kinase (JNK) (33), and tyrosine kinases (34). To obtain some insights into the signaling pathways involved in exposure of the N terminus of Bak in a caspase-8-independent fashion after Fas stimulation, we employed several kinase inhibitors to examine whether N-terminal exposure induced by CH11 in the presence of z-VAD-fmk could be blocked in HeLa cells. Among the inhibitors tested, PD98059 (ERK), SP600125 (JNK), and genistein (tyrosine kinases) did not affect Fas-induced caspase-8-independent exposure of the N terminus of Bak (data not shown). However, the pan kinase inhibitor staurosporine (STS) (10 nM) impaired the increase of anti-Bak Ab1 immunoreactivity induced by CH11 in the presence of z-VAD-fmk (Fig. 7*A*), although STS did not inhibit the increase of anti-Bak Ab1 immunoreactivity induced by CH11 alone (Fig. 7*A*). This indicates that at least two independent pathways are involved in exposure of the N terminus of Bak after Fas stimulation, one that is caspase-8/Bid-independent and involves an STS-sensitive kinase and another that is the well characterized caspase-8/Bid pathway. The inhibitory effect of STS was also confirmed by our *in vitro* permeabilized cell system. As shown in Fig. 7*B*, consistent with the *in vivo* results, cytosol derived from cells treated with CH11 in the presence of z-VAD-fmk together with STS could not induce exposure of the N terminus of Bak, whereas cytosol from cells treated with CH11 in the presence of z-VAD-fmk and rBid induced exposure of the N terminus. Furthermore, cytosol from cells treated with CH11/z-VAD-fmk/STS also failed to enhance rBid-induced cytochrome *c* release from isolated mitochondria (Fig. 7*C*). These results indicate that an STS-sensitive kinase plays a role in caspase-independent exposure of the N terminus of Bak after Fas stimulation.

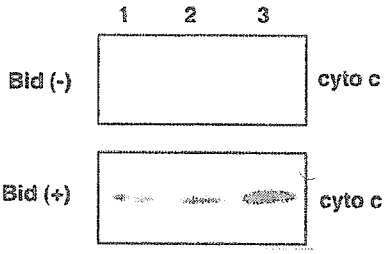

FIG. 5. **Enhancement of Bid-induced release of cytochrome *c* from isolated mitochondria by cytosol from cells with prior exposure of the N terminus of Bak.** Cytosol derived from untreated caspase-$8^{-/-}$ MEFs (*lane 2*) and caspase-$8^{-/-}$ MEFs treated with 0.5 μg/ml Jo2 for 16 h (*lane 3*) were incubated with mitochondria isolated from rat livers for 5 min, followed by incubation with (*lower panel*) or without (*upper panel*) rBid (30 μg) for a further 20 min. As a negative control, isotonic buffer was added instead of cytosol (*lane 1*). Release of cytochrome *c* was determined by Western blotting.

DISCUSSION

In response to various apoptotic stimuli, Bax and Bak undergo conformational changes such as exposure of their N terminus and homo-oligomerization: the homo-oligomers are considered to be active forms that induce permeabilization of the outer mitochondrial membrane, a process that is central to apoptotic death (3, 4). During death receptor-mediated apoptosis (type II cells), formation of the active forms of Bax and Bak depends on activation of caspase-8 and subsequent cleavage of Bid, because both caspase-8 and Bid are essential for these modes of apoptosis (11, 29, 35). In the present study, however, we showed that, in the absence of caspase-8 activa-

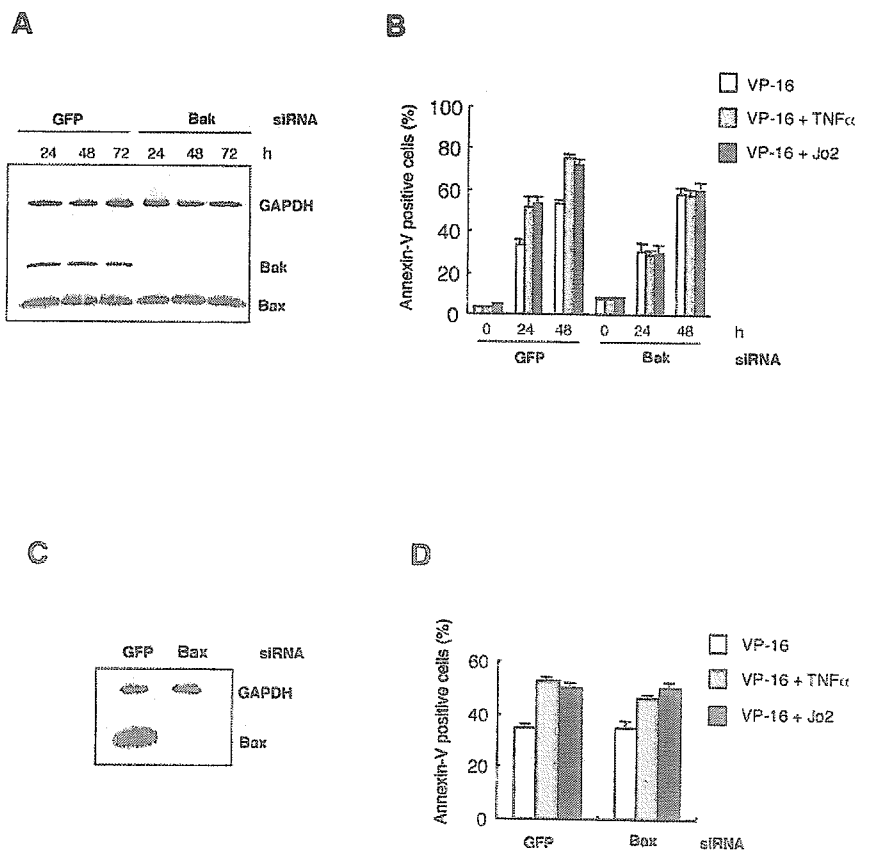

FIG. 6. **Requirement of Bak for the Jo2-induced increased susceptibility to VP-16 of caspase-$8^{-/-}$ MEFs.** *A*, caspase-$8^{-/-}$ MEFs were transfected with Bak siRNA (10 μg) or GFP siRNA (10 μg). Expression of Bak, Bax, and glyceraldehyde-3-phosphate dehydrogenase was detected at the indicated times after the last transfection of siRNA by Western blotting. *B*, siRNA-transfected caspase-$8^{-/-}$ MEFs were treated with Jo2 (0.5 μg/ml) or TNFα (10 ng/ml) for 16 h, followed by incubation with 10 μM VP-16 for the indicated times. Apoptotic cells were detected by Annexin-V staining. Data are shown as the mean ± S.E. (n = 3). *C*, caspase-$8^{-/-}$ MEFs were transfected with Bax siRNA (10 μg) or GFP siRNA (10 μg). Expression of Bax and glyceraldehyde-3-phosphate dehydrogenase was detected 24 h after the last transfection by Western blotting. *D*, siRNA-transfected caspase-$8^{-/-}$ MEFs were treated with Jo2 (0.5 μg/ml) or TNFα (10 ng/ml) for 16 h, followed by incubation with 10 μM VP-16 for 24 h. Apoptotic cells were detected by Annexin-V staining. Data are shown as the mean ± S.E. (n = 3).

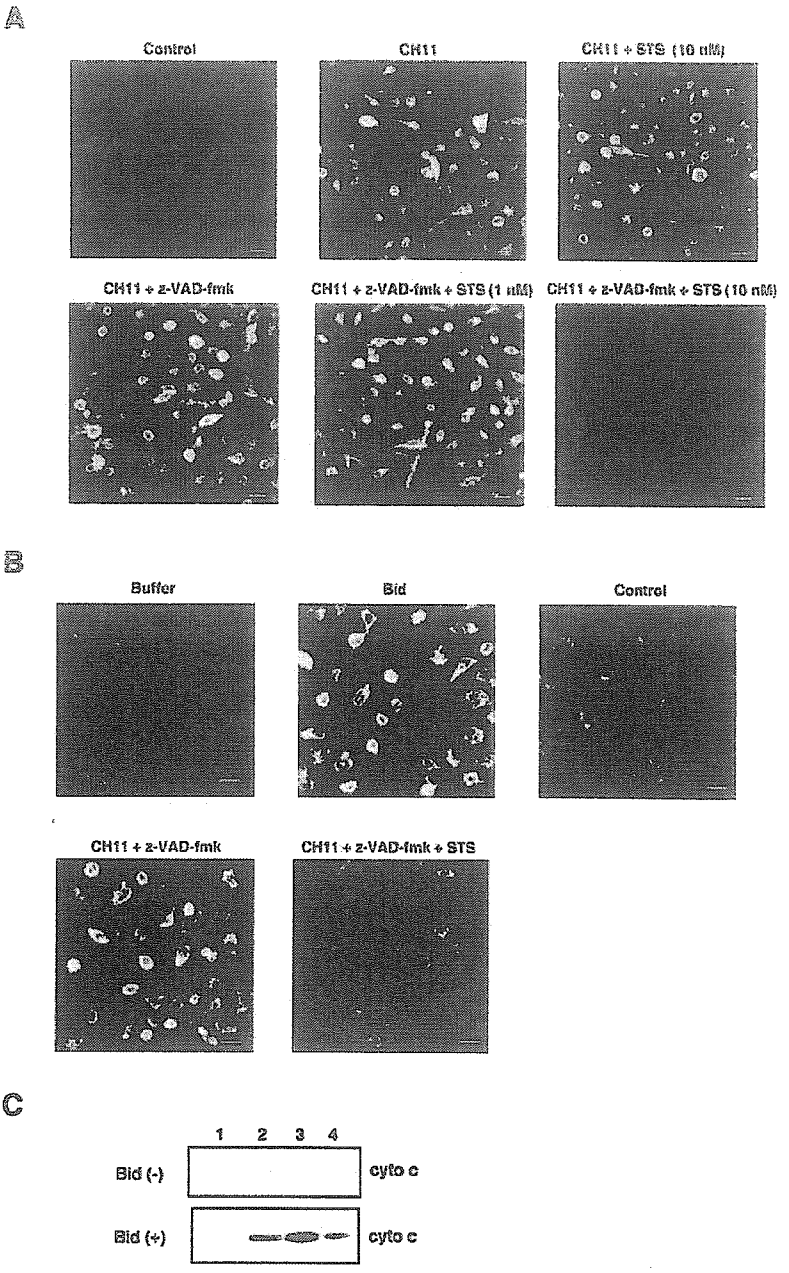

FIG. 7. **Inhibition by STS of caspase-8-independent exposure of the N terminus of Bak induced by Fas.** *A*, HeLa cells were treated as indicated for 2 h, and then were immunostained with anti-Bak Ab1 antibody. *Scale bar* = 20 μm. *B*, digitonin-permeabilized HeLa cells were incubated for 10 min with cytosol derived from HeLa cells with or without CH11/z-VAD-fmk treatment in the presence or absence of STS, followed by immunostaining with monoclonal anti-Bak Ab1 antibody. Isotonic buffer and rBid (0.5 μg) was added instead of cytosol as the negative and positive control, respectively. *Scale bar* = 10 μm. *C*, mitochondria isolated from rat livers were incubated for 5 min with isotonic buffer (*lane 1*), cytosol derived from untreated HeLa cells (*lane 2*), cytosol from HeLa cells treated with CH11 (0.5 μg/ml) and z-VAD-fmk (100 μM) in the absence (*lane 3*) or presence of STS (10 nM) (*lane 4*), followed by incubation with (*lower panel*) or without (*upper panel*) rBid (30 μg) for a further 20 min. Release of cytochrome *c* was detected by Western blotting.

tion, stimulation of Fas and TNF receptor still induced exposure of the N terminus of Bak, suggesting that N-terminal exposure and homo-oligomerization were separable, which is consistent in principle with the previous report that activation of Bak proceeds in multiple steps (19). Similar observations have also been reported for Bax (36, 37). Importantly, we also provided evidence that Bak with N-terminal exposure is in a primed state, because cells possessing Bak with N-terminal exposure were more sensitive to subsequent apoptotic stimulation. This may imply that exposure of the N terminus of Bax/Bak is a prerequisite for homo-oligomerization. Because it is known that exposure of the N terminus of Bax/Bak and oligomerization can be induced by tBid (11, 12), which is generated from Bid by active caspase-8 during death receptor-mediated apoptosis, it needs to be determined whether caspase-dependent exposure of the N terminus of Bak (induced via tBid) and caspase-independent exposure during death receptor-induced apoptosis are identical or not. It is also to be determined how significantly caspase-8-independent exposure of the N terminus of Bak contributes to death receptor-mediated apoptosis. This would be answered once a signaling molecule involved in this process has been identified.

In our present study, we found that Fas stimulation induced exposure of the N terminus of Bak not only in HeLa cells, but also in Jurkat cells. This does not seem consistent with the previous observation of Griffiths *et al.* (13). These authors showed that CH11 (1 ng/ml) could not cause exposure of the N terminus of Bak in Jurkat cells. This discrepancy may be due to a difference in CH11 concentration used. In fact, we found that exposure of the N terminus of Bak did not occur when CH11 concentration was lower than 10 ng/ml (data not shown), suggesting that exposure of the N terminus of Bak requires strong signals from death receptors.

What signals are elicited by stimulation of Fas and TNF

receptor, leading to caspase-8-independent exposure of the N terminus of Bak? Recently, caspase-10 has been identified as an alternative mechanism of death receptor-induced cell death (38). However, it is not likely that caspase-10 induced exposure of the N terminus of Bak, because the caspase inhibitor z-VAD-fmk could not suppress Fas-induced exposure of the N terminus in HeLa and Jurkat cells. Furthermore, the caspase-10 gene has not yet been identified in mice. It has been reported that engagement of Fas activates different signaling pathways, leading to activation of ERK (30–32), JNK (33), tyrosine kinase (34), or phosphatidylcholine-specific phospholipase C (39). It is possible that any of these caspase-independent signaling pathways could transmit a signal to mitochondrial Bak. The present study showed that a nonspecific protein kinase inhibitor, STS, actually inhibited Fas-induced exposure of the N terminus of Bak in the presence of z-VAD-fmk, but not inhibitors of ERK, JNK, or tyrosine kinases. Although further studies are necessary for identification of the kinase(s) responsible for Fas-induced caspase-8-independent exposure of the N terminus of Bak, our results indicate that stimulation of death receptors can elicit two independent signals targeting the mitochondria that regulate Bak activation, one via caspase-8/Bid and the other via a caspase-8-independent pathway that possibly involves one or more kinases.

In death receptor-induced apoptosis, activation of Bak is mainly mediated by the caspase-8/Bid pathway. Because we showed that Fas-induced caspase-independent exposure of the N terminus of Bak occurred in MEFs in the absence of cycloheximide, which was suggested to overcome the inhibitory effect of cFLIP or vFLIP on death-inducing signaling complex-dependent activation of caspase-8 (40), the caspase-independent signaling pathway that primes Bak might contribute to some death paradigms such as elimination of cells infected with vFLIP-producing virus by cooperation with other intrinsic apoptotic signals targeting the mitochondria.

In conclusion, a death receptor-activated caspase-independent signal induces exposure of the N terminus of Bak. Although this change is not sufficient for activation, it primes Bak for full activation. Thus, our results have revealed a novel signaling pathway involved in death receptor-mediated apoptosis.

Acknowledgment—We are grateful to Dr. S. Nagata for providing a caspase-8-deficient derivative of Jurkat (JB6).

REFERENCES

1. Wolf, B. B., and Green, D. R. (2002) *Curr. Biol.* **12,** R177–R179
2. Wang, X. (2001) *Genes Dev.* **15,** 2922–2933
3. Tsujimoto, Y. (2003) *J. Cell. Physiol.* **195,** 158–167
4. Danial, N. N., and Korsmeyer, S. J. (2004) *Cell* **116,** 205–219
5. Wei, M. C., Zong, W. X., Cheng, E. H., Lindsten, T., Panoutsakopoulou, V., Ross, A. J., Roth, K. A., MacGregor, G. R., Thompson, C. B., and Korsmeyer, S. J. (2001) *Science* **292,** 727–730
6. Lindsten, T., Ross, A. J., King, A., Zong, W. X., Rathmell, J. C., Shiels, H. A., Ulrich, E., Waymire, K. G., Mahar, P., Frauwirth, K., Chen, Y., Wei, M., Eng, V. M., Adelman, D. M., Simon, M. C., Ma, A., Golden, J. A., Evan, G., Korsmeyer, S. J., MacGregor, G. R., and Thompson, C. B. (2000) *Mol. Cell* **6,** 1389–1399
7. Scaffidi, C., Fulda, S., Srinivasan, A., Friesen, C., Li, F., Tomaselli, K. J., Debatin, K. M., Krammer, P. H., and Peter, M. E. (1998) *EMBO J.* **17,** 1675–1687
8. Luo, X., Budihardjo, I., Zou, H., Slaughter, C., and Wang, X. (1998) *Cell* **94,** 481–490
9. Li, H., Zhu, H., Xu, C. J., and Yuan, J. (1998) *Cell* **94,** 491–501
10. Desagher, S., Osen-Sand, A., Nichols, A., Eskes, R., Montessuit, S., Lauper, S., Maundrell, K., Antonsson, B., and Martinou, J. C. (1999) *J. Cell Biol.* **144,** 891–901
11. Wei, M. C., Lindsten, T., Mootha, V. K., Weiler, S., Gross, A., Ashiya, M., Thompson, C. B., and Korsmeyer, S. J. (2000) *Genes Dev.* **14,** 2060–2071
12. Eskes, R., Desagher, S., Antonsson, B., and Martinou, J. C. (2000) *Mol. Cell. Biol.* **20,** 929–935
13. Griffiths, G. J., Dubrez, L., Morgan, C. P., Jones, N. A., Whitehouse, J., Corfe, B. M., Dive, C., and Hickman, J. A. (1999) *J. Cell Biol.* **144,** 903–914
14. Hsu, Y. T., and Youle, R. J. (1998) *J. Biol. Chem.* **273,** 10777–10783
15. Antonsson, B., Montessuit, S., Sanchez, B., and Martinou, J. C. (2001) *J. Biol. Chem.* **276,** 11615–11623
16. Goping, I. S., Gross, A., Lavoie, J. N., Nguyen, M., Jemmerson, R., Roth, K., Korsmeyer, S. J., and Shore, G. C. (1998) *J. Cell Biol.* **143,** 207–215
17. Wolter, K. G., Hsu, Y. T., Smith, C. L., Nechushtan, A., Xi, X. G., and Youle, R. J. (1997) *J. Cell Biol.* **139,** 1281–1292
18. Cheng, E. H., Sheiko, T. V., Fisher, J. K., Craigen, W. J., and Korsmeyer, S. J. (2003) *Science* **301,** 513–517
19. Griffiths, G. J., Corfe, B. M., Savory, P., Leech, S., Esposti, M. D., Hickman, J. A., and Dive, C. (2001) *Oncogene* **20,** 7668–7676
20. Gross, A., Jockel, J., Wei, M. C., and Korsmeyer, S. J. (1998) *EMBO J.* **17,** 3878–3885
21. Antonsson, B., Montessuit, S., Lauper, S., Eskes, R., and Martinou, J. C. (2000) *Biochem. J.* **345,** 271–278
22. Shimizu, S., and Tsujimoto, Y. (2000) *Proc. Natl. Acad. Sci. U. S. A.* **97,** 577–582
23. Kawahara, A., Ohsawa, Y., Matsumura, H., Uchiyama, Y., and Nagata, S. (1998) *J. Cell Biol.* **143,** 1353–1360
24. Nomura, M., Shimizu, S., Ito, T., Narita, M., Matsuda, H., and Tsujimoto, Y. (1999) *Cancer Res.* **59,** 5542–5548
25. Shimizu, S., Eguchi, Y., Kamiike, W., Funahashi, Y., Mignon, A., Lacronique, V., Matsuda, H., and Tsujimoto, Y. (1998) *Proc. Natl. Acad. Sci. U. S. A.* **95,** 1455–1459
26. Mikhailov, V., Mikhailova, M., Pulkrabek, D. J., Dong, Z., Venkatachalam, M. A., and Saikumar, P. (2001) *J. Biol. Chem.* **276,** 18361–18374
27. Ruffolo, S. C., and Shore, G. C. (2003) *J. Biol. Chem.* **278,** 25039–25045
28. Cheng, E. H., Wei, M. C., Weiler, S., Flavell, R. A., Mak, T. W., Lindsten, T., and Korsmeyer, S. J. (2001) *Mol. Cell* **8,** 705–711
29. Varfolomeev, E. E., Schuchmann, M., Luria, V., Chiannilkulchai, N., Beckmann, J. S., Mett, I. L., Rebrikov, D., Brodianski, V. M., Kemper, O. C., Kollet, O., Lapidot, T., Soffer, D., Sobe, T., Avraham, K. B., Goncharov, T., Holtmann, H., Lonai, P., and Wallach, D. (1998) *Immunity* **9,** 267–276
30. Shinohara, H., Yagita, H., Ikawa, Y., and Oyaizu, N. (2000) *Cancer Res.* **60,** 1766–1772
31. Desbarats, J., Birge, R. B., Mimouni-Rongy, M., Weinstein, D. E., Palerme, J. S., and Newell, M. K. (2003) *Nat. Cell Biol.* **5,** 118–125
32. Lambert, C., Landau, A. M., and Desbarats, J. (2003) *Apoptosis* **8,** 551–562
33. Yang, X., Khosravi-Far, R., Chang, H. Y., and Baltimore, D. (1997) *Cell* **89,** 1067–1076
34. Eischen, C. M., Dick, C. J., and Leibson, P. J. (1994) *J. Immunol.* **153,** 1947–1954
35. Yin, X. M., Wang, K., Gross, A., Zhao, Y., Zinkel, S., Klocke, B., Roth, K. A., and Korsmeyer, S. J. (1999) *Nature* **400,** 886–891
36. Yethon, J. A., Epand, R. F., Leber, B., Epand, R. M., and Andrews, D. W. (2003) *J. Biol. Chem.* **278,** 48935–48941
37. Makin, G. W., Corfe, B. M., Griffiths, G. J., Thistlethwaite, A., Hickman, J. A., and Dive, C. (2001) *EMBO J.* **20,** 6306–6315
38. Kischkel, F. C., Lawrence, D. A., Tinel, A., LeBlanc, H., Virmani, A., Schow, P., Gazdar, A., Blenis, J., Arnott, D., and Ashkenazi, A. (2001) *J. Biol. Chem.* **276,** 46639–46646
39. Cifone, M. G., Roncaioli, P., De Maria, R., Camarda, G., Santoni, A., Ruberti, G., and Testi, R. (1995) *EMBO J.* **14,** 5859–5868
40. Krueger, A., Baumann, S., Krammer, P. H., and Kirchhoff, S. (2001) *Mol. Cell. Biol.* **21,** 8247–8254

THE JOURNAL OF BIOLOGICAL CHEMISTRY

Vol. 279, No. 41, Issue of October 8, pp. 42758–42764, 2004
Printed in U.S.A.

CA Repeats in the 3′-Untranslated Region of *bcl-2* mRNA Mediate Constitutive Decay of *bcl-2* mRNA* ♦

Received for publication, July 1, 2004
Published, JBC Papers in Press, August 3, 2004, DOI 10.1074/jbc.M407357200

Jung-Hee Lee‡, Mi-Hee Jeon‡, Yun-Jee Seo‡, Yong-Joon Lee‡, Jeong Heon Ko§, Yoshihide Tsujimoto¶, and Jeong-Hwa Lee‡‖

From the ‡Department of Biochemistry, The Catholic University of Korea, Seoul 137-701, Korea, the §Proteomics System Research Center, Korean Research Institute of Bioscience and Biotechnology, Daijeon 305-333, Korea, and the ¶Department of Post-genomics and Diseases, Osaka University Medical School and Solution Oriented Research for Sciences and Technology (SORST) of Japan Science & Technology Corporation (JST), Suita, Osaka 565-0871, Japan

An AU-rich element (ARE) in the 3′-untranslated region (UTR) of *bcl-2* mRNA has previously been shown to be responsible for destabilizing *bcl-2* mRNA during apoptosis through increasing AUF1 binding. In the present study, we investigated the effect of the region upstream of the ARE on *bcl-2* mRNA stability using serial deletion constructs of the 3′-UTR of *bcl-2*. Deletion of 30 nucleotides mostly consisting of the CA repeats, located upstream of the ARE, resulted in the stabilization of *bcl-2* mRNA abundance, in the absence or presence of the ARE. The specificity of the CA repeats in terms of destabilizing *bcl-2* mRNA was proven by the substituting the CA repeats with other alternative repeats of purine/pyriminine, but this had no effect on the stability of *bcl-2* mRNA. CA repeats alone, however, failed to confer instability to *bcl-2* or *gfp* reporter mRNAs, indicating a requirement for additional sequences in the upstream region of the 3′-UTR. Serial deletion and replacement of a part of the region upstream of the CA repeats revealed that the entire 131-nucleotide upstream region is an essential prerequisite for the CA repeat-dependent destabilization of *bcl-2* mRNA. Unlike the ARE, CA repeat-mediated degradation of *bcl-2* mRNA was not accelerated upon apoptotic stimulus. Moreover, the upstream sequences and CA repeats are conserved among mammals. Collectively, CA repeats contribute to the constitutive decay of *bcl-2* mRNA in the steady states, thereby maintaining appropriate *bcl-2* levels in mammalian cells.

Apoptosis is a tightly controlled cellular suicide program that is critical for the successful development of multicellular organisms, the maintenance of normal tissue homeostasis, and removal of damaged cells (1). The protooncogene *bcl-2*, originally isolated from the chromosomal breakpoint of a t(14, 18)-bearing B cell lymphoma, serves as an important repressor of apoptosis in a variety of cell types (2, 3). In line with its significant role in altering susceptibility to apoptosis, investigations of the mechanisms by which *bcl-2* expression is modulated may prove crucial for identifying therapeutic strategies for cancer and some neurodegenerative diseases and for defining the role of *bcl-2* in the development of multiple tissues (4).

Recent studies have indicated that *bcl-2* is regulated at both the transcriptional and posttranscriptional levels. A number of negative transcriptional regulatory sites have been described in the *bcl-2* promoter region (5, 6), and several transcription factors, including cAMP response element binding protein, A-Myb and WT1, are known to be involved in the positive regulation of *bcl-2* transcription (7–9). In addition to the promoter region, some sequences within the coding region, such as estrogen response elements, have also been demonstrated to mediate the transcriptional modulation of *bcl-2*, as was shown in breast cancer cell lines (10). The posttranscriptional modification of *bcl-2* includes the phosphorylation of Bcl-2 at the putative mitogen-activated protein kinase sites, which confers resistance against ubiquitination- and proteasome-dependent degradation (11, 12), and caspase-dependent cleavage, which results in the loss of anti-apoptotic activity (13, 14). Another mechanism of posttranscriptional regulation of *bcl-2* expression is based on mRNA stability. Recent reports have described that a conserved AU-rich element (ARE)[1] is present in the 3′-untranslated region (UTR) of *bcl-2* mRNA (15) and that interaction of ARE with a number of ARE-binding proteins, including AUF1, is associated with *bcl-2* mRNA decay during apoptosis (16, 17). In addition, transfection of a synthetic ribozyme targeting *bcl-2* ARE was shown to successfully down-regulate *bcl-2* mRNA expression accompanied by an increase in cell death in lymphoma cells (18), thus supporting the central role of ARE in the regulation of *bcl-2* gene expression.

A recent study using a cell-free *in vitro* degradation assay revealed that a 396-nt segment of the *bcl-2* 3′-UTR including the ARE was degraded faster than the ARE motif itself and that the 3′-UTR lacking the ARE was still degraded faster than control RNA (19). These findings suggest that, in addition to the ARE, other regulatory sites might exist in the 3′-UTR, upstream or downstream of the ARE. Here, we investigated the effect of the region upstream of the ARE on *bcl-2* mRNA stability and identified a new putative *bcl-2* mRNA destabilization determinant that contains CA repeats, mediating the constitutive decay of *bcl-2* mRNA.

EXPERIMENTAL PROCEDURES

Cell Culture and Transfection—The African green monkey kidney cells (COS7) were obtained from the American Type Culture Collection

* This work was supported by Grant R04-2002-000-00127-0 from the Basic Research Program of the Korea Science & Engineering Foundation. The costs of publication of this article were defrayed in part by the payment of page charges. This article must therefore be hereby marked "*advertisement*" in accordance with 18 U.S.C. Section 1734 solely to indicate this fact.

♦ This article was selected as a Paper of the Week.

‖ To whom correspondence should be addressed: Dept. Biochemistry, College of Medicine, The Catholic University of Korea, 505 Banpo-dong, Seocho-Gu, Seoul 137-701, Korea. Tel.: 82-2-590-1180; Fax: 82-2-596-4435; E-mail: leejh@catholic.ac.kr.

[1] The abbreviations used are: ARE, AU-rich element; 3′-UTR, 3′-untranslated region; CAR, CA-repeated region; Act D, actinomycin D; GFP, green fluorescence protein; DIG, digoxigenin; nt, nucleotide(s); GAPDH, glyceraldehyde-3-phosphate dehydrogenase; eNOS, endothelial nitric-oxide synthase.

and grown in Dulbecco's modified Eagle's medium supplemented with 10% heat-inactivated fetal bovine serum (Hyclone) and antibiotic solutions (100 units/ml penicillin and 100 μg/ml streptomycin, Invitrogen) under a 5% CO_2 humidified atmosphere at 37 °C. COS7 cells (1×10^6) were transfected in 6-well plates with 1 μg of plasmids using FuGENE 6 reagent (Roche Applied Science) according to the manufacturer's instructions. COS7 cells were harvested at 48 h after transfection for Northern and Western blotting. To evaluate mRNA degratation rates, further transcription was inhibited by adding actinomycin D (Act D) at 10 μg/ml (Sigma) 24 h after transfection, and then further incubating cells, before total RNA was extracted. To determine the degradation rate of *bcl-2* mRNA under apoptotic condition, 1 mM H_2O_2 was added to COS7 cells 1 h prior to treating Act D.

Plasmid Construction—A 1114-nt segment for the BU4 plasmid including the coding region (1459–2178) and 394 nt of the 3′-UTR was first obtained by PCR amplification using cDNA from HL60 cells as a template and corresponding primers flanked by an EcoRI restriction site (see Fig. 1A; all nucleotide positions were based on the sequence of accession number M13994 in GenBank™). The PCR products were purified from a 1% agarose gel and inserted into the TA cloning site of pGEM-T easy vector (Promega); sequences were confirmed by automated DNA sequencing. The EcoRI fragment was then subcloned in the EcoRI site of pCR3.1, named BU4. Other *bcl-2* cDNA constructs containing various lengths of the 3′-UTR were also produced by PCR using BU4 as a template for B, BU1, BU2, and BU3 and using BU3 for BU2-1, BU2-2, BU2-3, and BU2-4 with corresponding primers. For plasmids attached by other alternative repeats of purine and pyrimidine (BU2-2_{AT}, BU2-2_{CG}, BU2-2_{GT} and BU2-2_{CA}), reverse primers were designed to include five respective repeats at the last part, and BU2-2 was used as a template.

To prepare a chimeric cDNA, which contains a coding region of *bcl-2* and the 3′-UTR of unrelated gene followed by CA repeats ($BU3_{bis}$), two separate PCR amplifications were performed as follows. The first part confining the *bcl-2* coding region was synthesized with 5′-GAATTCATGGCGCACGCTGGGAGAACGGGG-3′ (forward, primer1) and 5′-GCTAGCTCACTTGTGGCTCAGATAGGCACC-3′ (reverse) flanked at the 5′-end by EcoRI and NheI restriction sites, respectively. The second part composed of 125 nt (1742–1866) in the 3′-UTR of the *bis* gene (GenBank™ accession number AF127139) and 30 nt of the CA-repeated region (CAR, 2310–2339) were PCR-amplified with forward primer 5′-GCTAGCCCTCTGCCCTGTAAAAATCAGACT-3′ and reverse primer 5′-GAATTCTGTGTGTGTGTGTCTGTCTGTGTGTGTGCACCCACGTTACTGC-3′ flanked at the 5′-end by NheI and EcoRI, respectively, using human *bis* gene (20) as a template. Each PCR product was independently cloned into pGEM-T easy vector and excised at the EcoRI and NheI sites for the first part and at the NheI and EcoRI sites for the second part. Two fragments were then ligated together into pCR3.1 at the EcoRI site to produce $BU3_{bis}$ construct in which 131 nt of the 3′-UTR of *bcl-2* was replaced with unrelated sequences including an NheI restriction site and part of the *bis* 3′-UTR. Two chimeric constructs of GFP, G2 and G3, were also prepared by ligating the two PCR products at the NheI and EcoRI sites as described above.

The 30 nt of CAR was directly inserted next to the stop codon (B_{CAR}) or following 42 nt ($B42_{CAR}$) or 82 nt ($B82_{CAR}$) of the 3′-UTR of *bcl-2* using 5′-GAATTCTGTGTGTGTGTGTCTGTCTGTGTGTGTGTCACTTGTGGCTCA-3′, 5′-GAATTCTGTGTGTGTGTGTCTGTCTGTGTGTGTGTAGTGAACCTT-3′, or 5′-GAATTCTGTGTGTGTGTGTCTGTCTGTGTGTGTGTATGGTACATC-3′ as reverse primers, respectively. The BU3-1, BU3-2, and BU3-3 constructs, in which a part of 131 nt in the 3′-UTR was replaced with unrelated sequences, were generated by ligating two PCR products using the XhoI site. The inserted sequence for the last 49 nt (BU3-3) is 5′-AATCAG**CAACTTCGTACCAGTAT(CTCGAG)ATCAGAACGTTGGAACT**TAT-3′ (the XhoI site is in parentheses). The underlined sequence was used to replace the first 42 nt (BU3-1) and the sequence in bold to replace for the middle 40 nt (BU3-2).

CAR was deleted from the 3′-UTR of BU4 plasmid ($BU4\Delta_{CAR}$) by a single step ligation of two the PCR products derived from BU4, upstream and down stream sequences of CAR, into the EcoRI sites of pCR3.1. Primer1 and 5′-CTCGAGGATGTTTATATGTGTGTTATTTTT-T-3′ containing a XhoI site (underlined) were used for the region upstream of CAR and 5′-CTCGAGCAATTAACAGTCTTCAGGCAAAA-C-3′ with a XhoI site (underlined) and 5′-GAATTCGGTGATCCGGCC-AACAAC-3′ with an EcoRI site (underlined) for the region downstream of CAR. Expression plasmids for mouse *bcl-2* were produced by PCR using cDNA from NIH3T3 cells and the primers corresponding to the various length of the 3′-UTR.

Northern Blot Analysis—Total RNA was extracted from cells using the RNAzol B reagent (Tel-Test Inc.), separated by electrophoresis through denaturing 2.2 M formaldehyde, 1% agarose gel, and then transferred onto positively charged nylon membrane by capillary blotting. Before blotting, 28 and 18 S ribosomal RNAs were visualized by ethidium bromide staining to ensure the integrity of the isolated RNA and to quantify RNA loading. RNA was UV cross-linked to the membrane, which was prehybridized for 1 h at 55 °C in high SDS hybridization buffer (5× SSC, 7% SDS, 50% formamide deionized, 0.1% *N*-lauroylsarcosine, 2% milk, and 50 mM sodium phosphate, pH 7.0), and then hybridized with digoxigenin (DIG)-labeled specified DNA probes, prepared by PCR labeling, in the same buffer at 55 °C overnight. The following primers were used to incorporate DIG-11 dUTP (Roche Applied Science) for different DNA probes; 5′-GGCAAGCTTGTGAACTGGGGGAGGATTGTG-3′ and 5′-GGCAAGCTTGAGCAGAGTCTTCAGAGACAG-3′ for *bcl-2*; 5′-TGAAGTTCATCTGCACCACC-3 and 5′-ACGAACTCCAGCAGGACCA-3 for GFP, and 5′-ACCACAGTCCATGCCATCAC-3′ and 5′-TCCACCACCCTGTTGCTGTA-3′ for GAPDH. The membrane was washed sequentially in 2× SSC, 0.1% SDS for 15 min at room temperature twice and in 0.1× SSC, 0.1% SDS for 15 min at 68 °C twice. Specific hybridization was then immunodetected with alkaline phosphatase-conjugated anti-DIG antibody (1:10,000, Roche Applied Science) followed by chemiluminescent substrate CDP-star (Roche Applied Science).

To determine the rate of *bcl-2* mRNA decay, total RNA was isolated from cells at multiple time points after treatment with Act D and then subjected to Northern blot analysis as described above. The membrane was stripped and rehybridized with GAPDH probe. The *bcl-2* mRNA signal was quantified at each time point by densitometry using Scion image software (Scion Corp.), normalized to GAPDH, and plotted as a percentage of the initial value against time.

Immunoblot Assay for Bcl-2 and Actin Proteins—Cells were lysed in RIPA buffer (50 mM Tris-HCl, pH 7.4, 150 mM sodium chloride, 1% Nonidet P-40, 0.5% sodium deoxycholate, 0.1% sodium dodecyl sulfate), and equal amounts of protein were separated by 12.5% SDS-PAGE followed by electrotransfer onto a polyvinylidene difluoride membrane (Milipore). The membranes were incubated with a monoclonal antibody to human Bcl-2 (Santa Cruz Biotechnology), GFP (Clontech), or β-actin (Sigma) and developed after incubation with horseradish peroxidase-conjugated secondary antibodies (Promega) using the enhanced detection system (Amersham Biosciences).

In Vitro Transcription—To examine the effect of the presence of the CA repeats in the 3′-UTR on the transcription of *bcl-2*, the transcripts of BU2 or BU3 constructs were synthesized *in vitro* using T7 RNA polymerase (21). BU2 or BU3 was first subcloned into the EcoRI site of pBluescript SK− in sense orientation with respect to the T7 promoter. *In vitro* transcripts were then synthesized using 0.5 μg of DNA linearized at the SpeI site with 20 units of T7 polymerase (Roche Applied Science) in transcription reaction buffer containing 20 units of RNase inhibitor and a 0.05 mM concentration each of ATP, CTP, GTP, and UTP for 2 h at 37 °C according to the manufacturer's instruction. After treatment of DNase I (Promega, 1 unit/reaction), the purity as well as the amount of RNA transcripts were determined by using 1% formaldehyde-agarose gel followed by ethidium bromide staining.

RESULTS

The CA Repeats in the 3′-UTR Contribute to the Destabilization of bcl-2 mRNA—To investigate the contribution of the sequence of the 3′-UTR upstream of the ARE of *bcl-2* to the stability of *bcl-2* mRNA, we prepared a series of 3′-UTR deletion mutants of *bcl-2* between its stop codon and the ARE by PCR, as shown in Fig. 1*A*. Each cDNA fragment-containing coding region and the indicated portion of the 3′-UTR was inserted into the pCR3.1 vector. The resulting constructs were transiently transfected into COS7 cells, and the level of *bcl-2* expression from each construct was analyzed by Northern and Western blotting. Fig. 1*B* shows that no significant differences of *bcl-2* expression were found in cells transfected with B, BU1, or BU2. However, the *bcl-2* mRNA level was lower in cells transfected with the BU3 cDNA than in cells transfected with B, BU1, or BU2 but was higher than in cells transfected with BU4 cDNA, which includes the ARE previously reported to be an apoptosis-dependent destabilizing element for *bcl-2* mRNA (15). Similar results were obtained in Western blotting assays of Bcl-2 protein expression levels (Fig. 1*B*). Since all constructs used in this experiment were cloned into the same pCR3.1

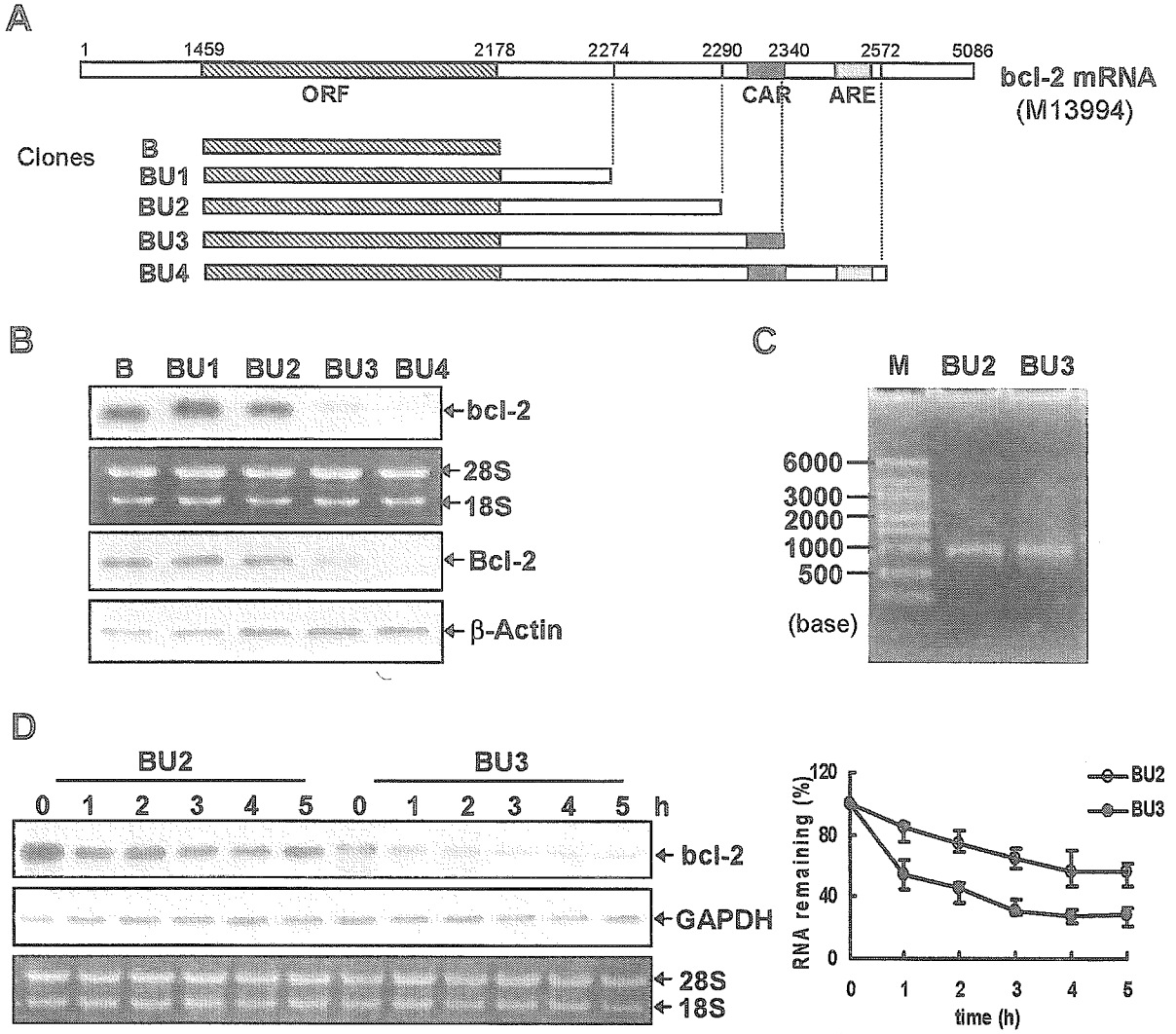

FIG. 1. **Regulation of *bcl-2* mRNA stability by a region upstream of ARE in the 3′-UTR.** *A*, schematic representation of five *bcl-2* constructs, which include various lengths of the 3′-UTR. The open reading frame (1459–2178) is shown as a *box* with *dashed lines*, and the previously reported ARE (2371–2465) is represented by a *gray box*. The *black box* indicates the CAR. The nucleotide sequence shown is based on the GenBank™ data base under accession number M13994. *B*, expression of *bcl-2* mRNA and Bcl-2 protein derived from various constructs shown in *A*. COS7 cells were transiently transfected with 1 μg of each constructs, and total RNA and protein were extracted after 48 h of transfection. Northern blot analysis was performed using 3 μg of total RNA using DIG-labeled *bcl-2* probe. Ethidium bromide-stained 28 and 18 S ribosomal RNAs were used as loading controls. Western blot analysis was performed in parallel with Northern blotting. One μg of the total protein was separated by 12.5% SDS-PAGE, transferred to a membrane, and probed with an anti-Bcl-2 monoclonal antibody followed by a β-actin antibody. *C*, *in vitro* transcription of the coding region and subsequent region of the 3′-UTR of BU2 and BU3 was performed as described under "Experimental Procedure." RNA was visualized by staining with ethidium bromide. *D*, comparison of *bcl-2* mRNA degradation mediated by 3′-UTR of BU2 and BU3 constructs. mRNA decay rates were determined by Act D chase experiments and Northern blotting. 24 h after transfection, 10 μg/ml Act D was added to COS7 cells, which were harvested at the indicated times for hybridization with the *bcl-2* probe, and subsequently with a GAPDH probe as a loading control (*left panel*). *bcl-2* mRNA remaining at each time point was plotted against time as a percentage of its initial value, after being normalized to GAPDH (*right graph*). Signal intensity at time 0 was defined as 100%. Results are shown as means ± of S.D. of three independent experiments.

vector, which has a cytomegalovirus promoter, the difference in the *bcl-2* mRNA level between BU2 and BU3 constructs was likely to be due to the differences in mRNA stability rather than differences in the transcription rate. Supporting our presumption, *in vitro* transcription experiments using T7 polymerase and BU2 or BU3 as templates revealed no significant difference in transcript level from each template (Fig. 1*C*).

We then compared the mRNA degradation rates of the transcripts from these two constructs by Act D chase experiments. Fig. 1*D* shows that the mRNA level of BU3 was reduced to 29% of the control at 5 h after adding Act D, while the mRNA level of BU2 was maintained at 56% of the control level, indicating that the BU3 mRNA was degraded faster than the BU2 mRNA. Therefore, these results suggest that the part of the 3′-UTR region present in BU3 but deleted in BU2 has the potential to affect *bcl-2* mRNA stability rather than the transcription processes.

To identify in detail the sequences with the mRNA destabilizing potential, the last 50 nt of the 3′-UTR sequences of the BU3 cDNA were serially deleted in 10-nt increments, and the expression levels of each construct were then compared by Northern blotting. As shown in Fig. 2*B*, transfection of the BU2-1 or BU2-2 construct, which, respectively, has 10 or 20 bases more than the BU2 construct, did not cause any decrease in the *bcl-2* mRNA level compared with BU2 cDNA. However, the mRNA level gradually decreased in the cells transfected with BU2-3, BU2-4, or BU3, which had serial additions of 10 nt, up to 30 nt. Interestingly, the sequences of these 30 nt (2311–2340), which dramatically reduced the *bcl-2* mRNA level, are mostly composed of CA repeats (+2 GA), indicating

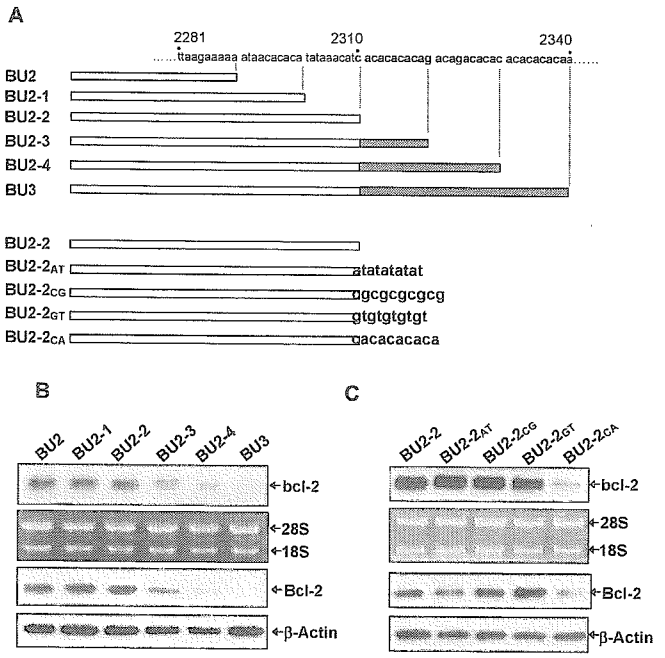

FIG. 2. **The *bcl-2* mRNA stability is regulated by CA repeats in the 3′-UTR.** *A*, schematic representation of the 3′-UTR of several *bcl-2* constructs. The coding region is not shown for convenience. The *upper panel* represents deletion mutants of 3′-UTR in which 10 nt were serially deleted from the 3′-end of the BU3 construct. The *lower panel* shows that five repeats of CA of BU2-3 were substituted with other purine-pyrimidine repeated sequences. *B* and *C*, Northern and Western blottings of *bcl-2* mRNA and protein, respectively, from deletion constructs, BU2, BU2-1, BU2-2, BU2-3, BU2-4, and BU3 (*B*) and from BU2-2, BU2-2_{AT}, BU2-2_{CG}, BU2-2_{GT}, and BU2-2_{CA} (*C*). Transfection and detection were performed as described in the legend to Fig. 1.

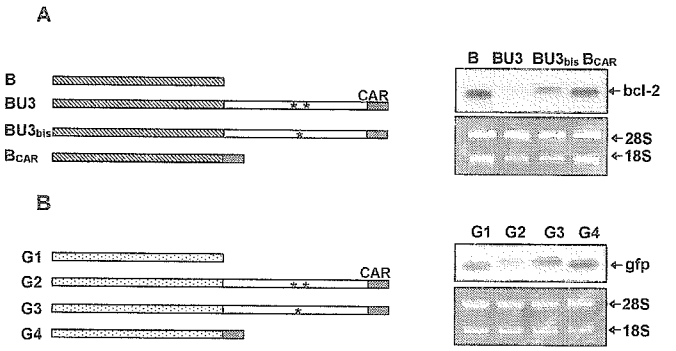

FIG. 3. **CA repeats are required but not sufficient for destabilization of *bcl-2* mRNA.** Schematic diagrams of *bcl-2* constructs (*A*) and GFP constructs (*B*) are shown in the *left panel* and the mRNA expressions of these constructs in the *right panel*. The coding region of the *bcl-2* and GFP genes are presented as *dashed* and *dotted boxes*, respectively. The $BU3_{bis}$ and G3 constructs include the 3′-UTR of the *bis* gene (*) and the CAR of the *bcl-2* gene, and G2 includes 131 nt of the 3′-UTR of the *bcl-2* gene (**), which was attached to the coding region of GFP. In B_{CAR} and G4 constructs, 30 nt of CA repeats was directly inserted into the 3′-end of the coding regions of *bcl-2* and GFP, respectively. Transfection and Northern blotting were carried out as described in the legend to Fig. 1.

that *bcl-2* mRNA stability decreased in proportion to the length of the CA repeats. We designated this region as CAR. It is notable that the BU2-3 construct, which has only five CA repeats, significantly reduced the *bcl-2* mRNA level. When the five repeats of CA in the BU2-3 cDNA were replaced with five repeats of AT, CG, or GT, as shown in Fig. 2*C*, the mRNA levels derived from these three constructs were similar to the mRNA level of the BU2-2 construct without the CA repeats, excluding the possibility that a simple repeat of purine and pyrimidine rather than sequence-specific CA repeats affect *bcl-2* mRNA stability.

Sequences Upstream of the 3′-UTR Are Required for CA Repeat-dependent Destabilization of bcl-2 mRNA—To establish whether the presence of CA repeats alone is sufficient to regulate *bcl-2* mRNA stability, we made two chimeric constructs, termed $BU3_{bis}$ and B_{CAR}, respectively, as indicated in Fig. 3*A*. Transfection with the B_{CAR} construct, in which 131 nt of the *bcl-2* 3′-UTR upstream of CA repeats were deleted, resulted in a marked stabilization of *bcl-2* mRNA despite the presence of the CA repeats, indicating an additional requirement of the proximal sequences of 3′-UTR for the CA repeat-dependent destabilization of *bcl-2* mRNA. Replacement of the proximal 131 nt of the *bcl-2* 3′-UTR with the unrelated sequences of 131 nt of the *bis* 3′-UTR also failed to destabilize *bcl-2* mRNA as efficiently as the 3′-UTR of *bcl-2*, even though a slight destabilization was observed. Therefore, it is not the simple distance between the stop codon and the CA repeats but the specific sequences in the 131 nt of the 3′-UTR that seem to confer the destabilizing potential of the CA repeats.

The destabilizing activity of the proximal region of the 3′-UTR of *bcl-2* was confirmed using a GFP reporter gene. The 3′-end of the open reading frame of the GFP cDNA was linked to the 131 nt of the 3′-UTR of *bcl-2* and subsequently to 30 nt of CA repeats, or directly to the CA repeats only, as described under "Experimental Procedures." Compared with the mRNA level expressed from the GFP coding region only, the insertion of 131 nt of the 3′-UTR together with CA repeats into the GFP coding region resulted in a comparable decrease in the GFP mRNA level, whereas insertion of the CA repeats only caused no decrease (Fig. 3*B*). The incorporation of 131 nt of the 3′-UTR of the *bis* gene, instead of the 3′-UTR of *bcl-2*, had no effect on *gfp* mRNA stability as in *bcl-2* mRNA, verifying the potential destabilizing activity of the 3′-UTR of *bcl-2*, which demands both the proximal 3′-UTR of *bcl-2* and subsequent CA repeats.

To determine the essential region affecting the CA repeat-dependent *bcl-2* mRNA destabilization, we attached 30 nt of CA repeats to 42 or 82 nt of the 3′-UTR of *bcl-2*. The *bcl-2* mRNA expressed from these two chimeric constructs showed significantly high levels, which corresponded to the mRNA levels from the construct in which all 131 nt were deleted (Fig. 4*A*). These results suggest that the last part of the 131 nt, lacking in these two constructs but present in the BU3 wild type, might be important for the CA repeat-dependent destabilization of *bcl-2* mRNA.

Subsequently, the last part of the proximal 131 nt of the 3′-UTR, as well as the first and middle part, were substituted with unrelated sequences. As shown in Fig. 4*B*, the replacement of each part increased *bcl-2* mRNA stability to a level similar to that of construct B, which contains only the coding region (Fig. 4*B*). These results, taken together, indicated that the overall mRNA structure provided by the linear sequences of the complete 131 nt of the 3′-UTR might be a prerequisite for the destabilizing ability of the subsequent CA repeats.

CA Repeat-dependent bcl-2 mRNA Destabilization Is Not Affected by Apoptosis—It has been reported previously that ARE-mediated decay in *bcl-2* mRNA is enhanced during apoptosis and that this is accompanied by increased binding of several AUBFs (15–17). To determine whether CA repeat-mediated *bcl-2* mRNA degradation also participates in the down-modulation of Bcl-2 during apoptosis, we investigated whether the degradation rate of *bcl-2* mRNAs with the 3′-UTR including the CA repeats but lacking ARE is affected by apoptotic stimulation. Act D chase experiments up to 5 h following transient transfection for 24 h revealed that the degradation of *bcl-2* mRNA with both CA repeats and ARE (BU4) was significantly accelerated by H_2O_2 treatment (Fig. 5, *B* and *central panel* of

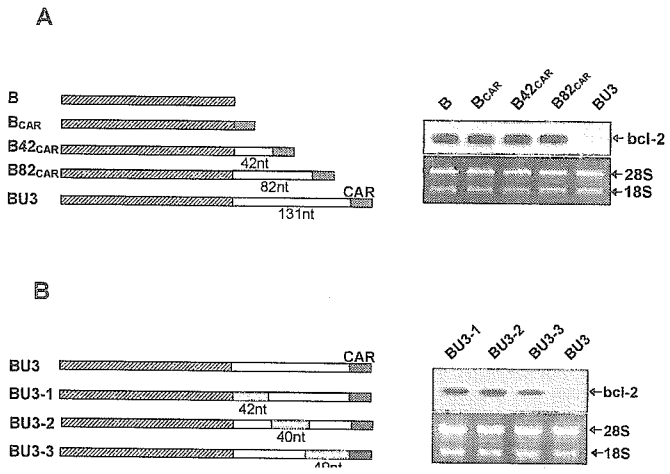

FIG. 4. **CA repeat-dependent destabilization of *bcl-2* mRNA requires sequences upstream of the CA repeats.** The upstream region to CA repeats was sequentially deleted (*A*) or replaced in part by unrelated sequences (*B*) as shown in the *left panel*. *Gray boxes* represent the substituted regions. The constructs were transfected into COS7 cells and Northern blotting was performed. 18 and 28 S were stained with ethidium bromide as RNA loading controls.

C), which is consistent with the earlier observation (15). However, the *bcl-2* mRNA with the CA repeats but lacking the ARE (BU3) was degraded at similar rates in the absence or presence of H_2O_2 to 38 or 33%, respectively, after treatment with Act D for 5 h, indicating that apoptotic conditions did not influence *bcl-2* mRNA decay mediated by CA repeats (Fig. 5, *B* and *left panel* of *C*). We also examined the decay of *bcl-2* mRNA with the ARE but not the CA repeats ($BU4\Delta_{CAR}$). Deletion of the CA repeats led to marked stabilization of *bcl-2* mRNA levels in the steady state, despite the presence of the ARE, but greatly enhanced the degradation of *bcl-2* mRNA following H_2O_2 treatment, as was revealed by a reduction in the remaining RNA from 107% to 35% after 5 h of Act D treatment (Fig. 5, *B* and *right panel* of *C*). These results, taken together, indicated that the degradation of *bcl-2* mRNA under apoptotic conditions was mainly mediated through the ARE component and that the CA repeats in the 3′-UTR may contribute to the constitutive decay of *bcl-2* mRNA.

Effect of CA Repeats on Mouse bcl-2 mRNA Stability—Whereas the ARE in the 3′-UTR of the *bcl-2* gene has been reported to be highly conserved in the human, mouse, chicken, and nematode (15), the CA repeats are confined to the 3′-UTRs of mammalian *bcl-2* genes. CA repeats in mouse *bcl-2*, located 115 nt from the stop codon, include 23 repeats of CA without G, and the sequences upstream of the CA repeats share 79% of homology with those of human *bcl-2* (Fig. 6*A*). To investigate whether CA repeats present in the 3′-UTR of the *bcl-2* genes of other species also exert destabilizing activity on its mRNA, we compared the mouse *bcl-2* mRNA levels from three different constructs. The mouse *bcl-2* gene with only coding sequences expressed a higher level of *bcl-2* mRNA compared with the mouse *bcl-2* mRNA with 161 nt of the 3′-UTR including the CA repeats. In addition, a 46-nt deletion of the CA repeats resulted in the marked stabilization of *mbcl-2* mRNA (Fig. 6*B*), as seen in human *bcl-2* mRNA. Therefore, the mRNA destabilizing ability of CA repeats in the 3′-UTR of *bcl-2* appears to be preserved among mammals to maintain *bcl-2* mRNA levels in various cellular environments.

DISCUSSION

ARE-mediated mRNA decay has recently been implicated in the regulation of *bcl-2* mRNA stability, which is activated by an apoptotic program (15–17). In this study we found that *bcl-2* mRNA decay is also modulated in part by the CA repeats in the 3′-UTR, which are located about 131 nt from the stop codon and upstream of the previously characterized ARE. The destabilizing potential of the CA repeats was confirmed by deleting the CA repeats from the 3′-UTR of *bcl-2*, which resulted in a marked increase in the level of *bcl-2* mRNA despite the presence of the ARE sequence (Fig. 5). These results suggest that the CA repeat is a novel determinant of *bcl-2* mRNA decay, which is in line with the previous finding that an ARE-deficient 3′-UTR of *bcl-2* was still degraded faster than control 3′-UTR *in vitro*, suggesting the presence of an additional *bcl-2* mRNA decay-regulatory element in the 3′-UTR (19). Therefore, the destabilizing activity of the 3′-UTR of *bcl-2* including the ARE demonstrated in earlier studies, which primarily focused on the ARE as a representative *bcl-2* mRNA destabilizing determinant, seems to be attributable not entirely to the ARE but substantially to CA repeats as well.

CA repeats are the most common dinucleotide polymorphism found in the human genome and thus are routinely used as genetic markers of allelic variants in various genes (22–24). Recently, a number of reports have described a correlation between the reduced expression levels of several genes such as IFN-γ and HSD11B2 and either the presence of repeats or an increase in the length of the repeats in the intron, suggesting a regulatory function of CA repeats on the processing of pre-mRNAs (25–27). Furthermore, CA repeats in intron 13 of the human endothelial nitric-oxide synthase (eNOS) gene seem to specify the cleavage site of the pre-mRNA of eNOS for splicing or degradation, depending on the presence of heterogeneous nuclear ribonucleoprotein L (hnRNPL) (28, 29). However, little is known about the functional importance of CA repeats in the exonic context. Here we describe for the first time that CA repeats in the 3′-UTR can target *bcl-2* mRNA for selective degradation, extending the role of CA repeats as an important element for modulating the stability of mRNA as well as the stability of pre-mRNA.

The mechanism by which CA repeats in an exon exert a negative effect on *bcl-2* mRNA abundance has not been clarified. However, exonic CA repeats for mRNA destabilization appear to involve a different pathway from that of intronic CA repeats for specifying the cleavage sites of the pre-RNA of eNOS, given that the CA repeats did not function as a splicing enhancer when moved in an exonic context (28). Furthermore, CA repeats were shown to be sufficient for the cleavage of eNOS pre-mRNA (29), whereas CA repeats were found to be essential but not sufficient to destabilize *bcl-2* mRNA, as shown by our results indicating that the incorporation of the CA repeats directly into the 3′-end of coding sequences of *bcl-2* or GFP mRNA did not affect mRNA stability (Fig. 3, *A* and *B*). On the other hand, levels of GFP reporter gene mRNA decreased after introduction of the proximal 131 nt and subsequent CA repeats of the 3′-UTR of *bcl-2*, whereas the incorporation of the same length of the 3′-UTR of the *bis* gene with the CA repeats had no effect on GFP or *bcl-2* mRNA stability. Finally, our deletion and replacement experiments indicate that the entire 131 nt region preceding the CA repeats is apparently a requisite for the destabilizing activity of the CA repeats (Fig. 4, *A* and *B*).

In addition to the requirement of the upstream sequences of the 3′-UTR, CA repeat-mediated decay of *bcl-2* mRNA was found to exhibit features that differed from ARE-mediated processes in several respects. The ARE in the 3′-UTR of *bcl-2* has been known to mediate *bcl-2* mRNA decay during apoptosis, either by increasing binding of destabilizing factors such as AUF1 (16, 17) or by reducing interaction with stabilizing factors such as nucleolin (30, 31). Our results show that the decay